NT

NATIONAL AERONAUTICS AND SPACE ADMINISTRATION

MSC INTERNAL NOTE NO. 68-FM-54

February 27, 1968

68-FM-54

PRELIMINARY ANALYSIS OF MONITORING AN IGM-STEERED, HYPERSURFACE-TARGETED TLI MANEUVER USING CMC LAMBERT STEERING AND THE SATURN-PREFERRED IMU ALIGNMENT

By Robert F. Wiley,
Lunar Mission Analysis Branch

MISSION PLANNING AND ANALYSIS DIVISION

MANNED SPACECRAFT CENTER
HOUSTON, TEXAS

MSC INTERNAL NOTE NO. 68-FM-54

PROJECT APOLLO

PRELIMINARY ANALYSIS OF MONITORING AN IGM-STEERED, HYPERSURFACE-TARGETED TLI MANEUVER USING CMC LAMBERT STEERING AND THE SATURN-PREFERRED IMU ALIGNMENT

By Robert F. Wiley
Lunar Mission Analysis Branch

February 26, 1968

MISSION PLANNING AND ANALYSIS DIVISION
NATIONAL AERONAUTICS AND SPACE ADMINISTRATION
MANNED SPACECRAFT CENTER
HOUSTON, TEXAS

Approved: _____
M. P. Frank III, Chief
Lunar Mission Analysis Branch

Approved: _____
John P. Mayer, Chief
Mission Planning and Analysis Division

FIGURES

PRELIMINARY ANALYSIS OF MONITORING AN IGM-STEERED HYPERSURFACE-TARGETED TLI MANEUVER USING CMC LAMBERT STEERING AND THE SATURN-PREFERRED IMU ALIGNMENT

By Robert F. Wiley

SUMMARY

A preliminary investigation was made into the monitoring of the hypersurface-targeted, IGM-controlled TLI burn. The effect of dispersions in the EPO and thrust and specific impulse dispersions on the behavior of the monitoring parameters was studied. The TLI burn was simulated by the point mass, three-dimensional simulation in the ARM computer program using the Saturn-preferred alignment.

The monitoring parameters were the velocity-to-be-gained, total inertial attitudes, attitude rates, and attitude errors. The attitude errors were computed by subtracting the Lambert's cross-product-steering-commanded attitudes from the IGM-commanded attitudes.

The most important preliminary conclusion indicated by the results is that attitude errors are more meaningful to monitor than the total attitudes or rates. A more sophisticated simulation is necessary to conclusively prove this.

INTRODUCTION

This study was a preliminary investigation into onboard monitoring of the IGM-controlled TLI burns of Missions E and G within the capabilities of the ARM computer program. The program was altered to compute the CMC Lambert-targeted, cross-product steering commands and velocity-to-be-gained (V_g) as the burn was being simulated using the IGM. EPO and engine performance dispersions were considered to investigate their effects on the monitoring parameters. Only one IMU alignment, termed the Saturn preferred, was used; this study was <u>not</u> designed to show the monitoring characteristics of different IMU alignments. It was desired to draw conclusions about the worth of attitude error monitoring, to become familiar with the representative values of the monitoring parameters, to see what might or might not be meaningful parameters to monitor, and to raise questions about TLI monitoring.

Since this was only a preliminary study, it was not very comprehensive. Several dispersions occurring in the same burn were not investigated. Only the most probable method of IGM targeting, the onboard hypersurface, was used. With the hypersurface, the outgoing plane is redefined onboard for off-nominal EPO's. There is another method of IGM targeting that does not redefine the outgoing plane onboard; this alternate IGM targeting method was not studied. No catastrophic failures were studied to compare the monitoring characteristics' differences from nominal. Different state vectors in the CMC and Saturn computer were not simulated. References 1 and 2 show that this latter problem is serious for boost into EPO because of the desired end conditions. While the end conditions for TLI are not like those of EOI, this problem might still be serious for TLI.

Due to ARM programing errors it was not possible to simulate several dispersions. A difference between the actual vehicle mass and the mass used in computing guidance commands could not be simulated (i.e., the vehicle mass uncertainty at TLI could not be simulated). It was also impossible for the vehicle to compute its initial alignment as if the engine were going to perform nominally but have off-nominal engine performance (i.e., when there was to be a dispersed thrust level, the vehicle made an off-nominal alignment).

The important assumptions used in generating the data presented in this study are listed here:

1. The vehicle is considered a point mass; i.e., the simulation is three-dimensional. There is no bending, sloshing, or propellant utilization model. Any differences in the sensed motion of the vehicle due to the differences in position of the sensors is not simulated.

2. There is no DAP simulation.

3. There is perfect center-of-gravity knowledge.

4. The state vector going to the guidance is updated using all perturbing influences.

5. The same state vector is used to compute the IGM and cross-product guidance commands at each computing step (see flow chart).

NOTATION

ARM	Apollo Reference Mission (computer program)
IGM	iterative guidance mode
V_g	velocity-to-be-gained
EPO	earth parking orbit
CMC	command module computer
EOI	earth orbit insertion
RTCC	Real-Time Computer Complex
DAP	digital autopilot
IMU	inertial measurement unit
TLI	translunar injection

ANALYSIS AND RESULTS

Pitch, yaw, pitch rate, yaw rate, pitch and yaw errors, and V_g are shown in figures 4 through 23. The pitch and yaw errors were computed by subtracting the CMC Lambert cross-product-steering-commanded pitch and yaw from the actual vehicle (i.e., the IGM-commanded) pitch and yaw. Since the IGM guidance and steering is fundamentally different from the Lambert-guided, cross-product steering, it is not obvious that attitude errors will be meaningful parameters to monitor, especially in off-nominal situations. Therefore, the attitude errors were of special concern.

It should be pointed out initially that the dispersions that could be considered were limited due to the S-IVB restart logic not being available in ARM and several ARM programing errors (discovered after the data had been generated). Consequently some of the data obtained is not what would be expected in real time. However, it has been presented since it illustrates important points and can be used to draw conclusions.

The nominal Saturn-controlled TLI burn for both missions was done by the IGM using the hypersurface to generate IGM targets. The Mission E nominal was the old AS-503 reference trajectory burn. The Mission G nominal was the old AS-504 preliminary reference trajectory burn. The nominal burn characteristics are:

	Apogee altitude, n. mi.	Perigee altitude, n. mi.	Plane change, deg	ΔV, fps
Mission E	3 963.59	104.70	0.008	4 127.06
Mission G	311 485.65	112.96	2.590	10 509.51

Dispersions Considered

Tables I and II summarize the dispersions considered. The reasons for considering these dispersions are given here.

The ARM program does not simulate the S-IVB restart logic. Consequently the ignition time as well as the hypersurface parameters must be input to generate the IGM targets. Normally, the ignition time is determined onboard. A position vector, $\underline{S}$, is computed β degrees down-range in the EPO every second when the S-IVB is ready to start testing for reignition (see fig. 1). The angle α_{TS} between $\underline{S}$ and a premission-determined target vector $\underline{T}$ is computed for each $\underline{S}$. When the angle α_{TS} becomes equal to or greater than a value computed onboard, the burn is started and the outgoing conic plane is determined. This outgoing plane is defined by $\underline{S}$ and $\underline{T}$; therefore the plane will change if EPO dispersions are present since $\underline{S}$ will change. We need to see what effect EPO dispersions will have on monitoring. For example, if the CMC targets were placed onboard when the spacecraft is on the pad and were not updated, the spacecraft would be targeted to a different outgoing conic than the Saturn if any EOI errors were present. Since the ARM program does not simulate the restart logic, dispersions in the position and velocity components of the EPO at the nominal ignition time were made to change the outgoing conic. Note here that the mission E ignition state dispersions were done in the plumbline system and the mission G dispersions were done in the geocentric inertial system. Table II shows the geocentric inertial dispersion equivalent to each plumbline dispersion.

Table III gives α_{TS} and the wedge angle between the nominal and dispersed EPO's for these ignition state dispersions. A valid simulation of the restart would have α_{TS} greater or equal to the nominal α_{TS}. This

occurs in three of the five dispersed cases. One of the remaining two cases misses α_{TS} in the sixth decimal point, so calling this a bad simulation of a restart is really splitting hairs.

The two cases where α_{TS} is less than nominal should have different ignition times than those used in this study. For the different ignition times, the attitude errors could be worse than those presented here due to the time of flight used in the cross-product guidance.

The three good restarts are realistic simulations of the actual system. The angular velocity of a vehicle in a 100-n. mi. circular orbit is about 0.07 deg/sec. Thus, with a 1-second sampling rate on α_{TS}, α_{TS} could be greater than nominal by as much as 0.07°. Note that the dispersed α_{TS}'s do not exceed this limit.

It will be seen, when looking at the data, that these dispersions in the ignition state (or really the small differences between the hypersurface-computed outgoing conic and the one to which the CMC is targeted) will noticeably affect the monitoring. Thus the 1-second sampling rate on α_{TS} should be checked to see what effect it has on monitoring. To do this, the mission G burn was started 3 seconds late in EPO. Here α_{TS} was about 0.2° greater than the nominal.

The most obvious dispersions are those of thrust and specific impulse during the burn. The data presented in the appropriate figures between 4 and 23 on the attitudes and rates were obtained using the thrust and specific impulse models of figures 2 and 3. This data shows the differences between the models and a constant thrust and specific impulse burn flying to the same plane change and energy. The altered ARM program used in this study would not give attitude errors when the models were used. Consequently, the attitude errors were generated using a dispersed constant thrust and specific impulse. The difference from nominal ($\pm$30 000 lb of thrust) is an unreasonable figure. The logic for choosing a value this bad was that if the monitoring behaved for these cases it should also behave for more reasonable ones. This bad a dispersion will also give a radically different powered flight path; thus tentative conclusions about DAP effects can be drawn. As previously stated, the Saturn was aware of the coming dispersions and aligned itself differently from nominal. This means that the attitude and attitude errors are measured from an alignment that has compensated for the dispersion. If the IGM had not been aware of the dispersions to come, a different attitude and possibly different attitude errors would have resulted.

Alignment.- The IMU X-axis was placed along the IGM-computed ignition thrust acceleration vector, $\underline{a}_T$. When the IGM knows that a dispersion, such as a thrust dispersion, is coming and computes an off-nominal initial $\underline{a}_T$ to compensate, this becomes the new X-axis. The Y-axis was along $\underline{a}_T \times r$, where r is the radius at ignition, and the Z-axis completed the right-hand, orthogonal system. This has been called the Saturn-preferred alignment since the spacecraft-preferred alignment is exactly like this except the spacecraft $\underline{a}_T$ is used. Pitch, yaw, and roll are measured in this system as Euler angles to go from the initial alignment to the present alignment. If the alignment is not this Saturn-preferred one, the author is not certain if the attitude error curves will change. Of course, the attitudes themselves will change due to the coupling between pitch, yaw, and roll.

Initial attitude errors.- Reference 3 indicates that, in a CMC-controlled burn, there will be no initial attitude errors for two reasons. First, the IMU alignment is taken as the zero point for attitude reference. Second, the cross-product steering commands are not in the guidance loop for the first few seconds. The author is not certain that this same philosphy will be followed in the CMC monitoring of a TLI burn, but it is reasonable to assume that it will be[a]. Therefore, on the figures presented to show the attitude errors resulting from this study, the first 10 seconds have been left blank since it is still not certain if there will be initial attitude errors or not.

Spacecraft targeting.- The targets used here for monitoring may also be used in CMC control of the burn. There was one type of targeting used for the Mission G burn - that planned in the RTCC for CMC control of the burn (ref. 4). There were two types of Mission E targeting. The first, called IGMBO targeting, used the nominal IGM burnout conic orbit to select the target vector and time of flight. The only difference between this and the RTCC targeting is that the target vector was chosen at a true anomaly of 270° in the IGMBO case instead of 150° as in the RTCC. The second type of targeting, called GPMP targeting, was an impulsive maneuver type of targeting as described in reference 5. Since GPMP has the target vector at 270°, the IGMBO targeting target vector was also selected at 270° since the sensitivity of each targeting in monitoring was the main point to be studied. The cross-product steering constant, c, was equal to 1.00 in all three cases. For the presentation of the Missions E and G results together, the IGMBO targeting results were selected. Note that the Mission G targeting and Mission E IGMBO targeting force the nominal attitude errors to zero at the end of the burn since the cutoff conditions were used to generate the spacecraft targets.

---

[a]It could possibly be arranged to have initial attitude errors on display for TLI monitoring if the ground could tell the crew what to expect, either through an RTCC program or preflight data. This might be helpful, but nothing has been done to see how helpful.

Discussion of the Figures

The results are presented in figures 4 through 23. The nominal curve is presented on each graph for the particular quantity considered.

There is a method to the notation madness. In comparison of the two types of Mission E spacecraft targeting, the numbered curves are the IGMBO targeting curves; the lettered curves are the GPMP targeting curves. When results for both missions are presented together, the numbered curves are still Mission E, IGMBO targeted, while the lettered curves become Mission G.

It was mentioned earlier that the vehicle mass uncertainty at TLI could not be simulated; the IGM was aware of the actual mass. In real time, an off-nominal mass in EPO causes the onboard system to change the ignition time to one other than nominal. Pitch, yaw, and pitch and yaw errors were computed for $\pm$1500 lb at the nominal ignition time, in the nominal EPO, with nominal engine performance; the pitch profile differed from nominal by $\pm 1.5^{\circ}$, while the attitude error differences were small. Thus it is fortunate that an ignition time change is made for known mass differences. This data is not shown graphically in this note because the note is already large and cumbersome.

The attitude error and V_g curves for the low thrust, high specific impulse dispersion for Mission G go off the time scale. The time scale was not adjusted because it was desired to keep all time scales the same for easier comparison of the data.

A word is in order about the maximum nominal pitch and yaw errors for both missions. The Mission G maximum yaw error is greater than the maximum pitch error. This is believed to be because the cross-product pitch steering is more like the IGM than the cross-product yaw steering is. Note that the maximum yaw error for Mission G is approximately equal to the plane change. This is not so in Mission E; the maximum yaw error is greater than the plane change. This may be because of target vector placement or the nature of the IGM Mission E burn. This will be resolved by Mission E TLI monitoring data using the RTCC CMC targeting.

The graphs of the attitude rates, figures 19 through 23, show large fluctuations at the ends of the burns. This occurs where the IGM guidance freezes attitudes, and the magnitude is possibly due to the computing interval.

The computing step was 5 seconds on all cases except the thrust and specific impulse model cases where it was 1 second and where none of the fluctuations were seen at the end of the burn. However, these fluctuations are in the Boeing launch vehicle trajectory documents where plumbline attitudes are shown; thus these fluctuations could be authentic. This problem will be resolved as more TLI burns are done.

The comments on the V_g curves can be made together. It would be very hard to get into a situation where V_g would not decrease (e.g., the vehicle pointed 180° away from its nominal direction). The data here indicates that the crew would have trouble telling if V_g were behaving properly, unless a very close check against a nominal were kept. Thus, the crew would have noticed something was wrong before they noticed a bad V_g behavior. Consequently it can be concluded that V_g is an ineffective parameter tc monitor. The display space now used for V_g might be better used for something like the rate of change of altitude, the instantaneous perigee altitude, or time to perigee. The initial V_g may be of some use, but that display can be called up preburn. As an aside, note that the initial nominal V_g is not equal to the final ΔV of the burn:

	V_g Initial	ΔV Final
Mission E	4 180.62	4 127.06
Mission G	11 004.02	10 509.51

The comments on the 3-second ignition delay in Mission G can also be lumped together. The data indicates that the 1-second sampling rate in α_{TS} would have negligible effect on monitoring since the 3-second ignition delay has a small effect. Any deviations from nominal due to the 1-second α_{TS} sampling rate should be swamped by other dispersions.

Figure 8(a) - Inertial yaw error history for dispersed ignition states for the two Mission E targeting schemes.- The author cannot give any reason for the behavior of the 0.01-km/sec curve, especially with GPMP targeting.

Figure 8(b) - Inertial yaw error history for an out-of-plane position dispersion of the ignition state for the two types of Mission E targeting schemes.- A dispersion of 10 km out of plane would probably be taken out by a state vector update or else compensated for by an update of the spacecraft targets. This data shows one reason for doing this. It also illustrates how going out to a different conic than the CMC-targeted one can hurt the attitude errrors in Mission E.

Figure 12(a) - Inertial pitch history for dispersed ignition states for Missions E and G.- Since this is the first time the pitch histories have been shown in this note, a word of explanation is in order. If the vehicle were to hold attitude with respect to the local horizontal, it would experience an inertial pitch rate of about -0.07 deg/sec, which would give -7° of inertial pitch after 100 seconds. Both the Mission E and Mission G burns pitch up with respect to the local horizontal, giving a total inertial pitch at 100 seconds of less than 7°. In Mission G, at around the 250-second mark, the guidance terminates this pitch and begins a pitch down with respect to the local horizontal; it is here that the majority of energy is added to the vehicle orbit and the inertial pitch curve changes slope radically. This does not happen in Mission E.

Figure 12(b) - Inertial pitch error history for dispersed ignition states for Missions E and G.- There are basic differences between the spacecraft steering and IGM steering. The CMC does not change its pitch commands as the IGM does. Thus there should be some pitch errors. Note on the Mission G nominal curve that, where the IGM changes pitch objectives (at around 250 seconds), the pitch error curve reaches a peak. The author is not presently aware of any significance to the zero pitch error crossing at 173 seconds. The Mission E nominal pitch error curve does not follow the shape of the Mission G curve in that it crosses zero very late in the burn. This may be due to the different natures of the two IGM-controlled burns, but the different target vector placements for the spacecraft targeting may also be the reason. Monitoring data for Mission E TLI using the RTCC targeting scheme for the spacecraft will resolve this issue.

Figure 14(a) - Inertial pitch history for the two thrust and specific impulse models in Mission G.- Curves for Mission E using the two thrust and specific impulse models are not shown here. This is because the results obtained seemed grossly unreasonable. The high thrust and low thrust curves do not form an envelope of expected total pitch. This is because the initial alignment, to which these numbers are referenced, are different for the high, low, and nominal thrust levels.

Figure 14(b) - Inertial pitch error history for constant thrust and specific impulse dispersions for Missions E and G.- Because a large, constant thrust dispersion was used here, large inertial pitches were encountered. The error fluctuation in the vicinity of 60 seconds on Mission G occurs around the termination of these large inertial pitches. These curves show three things:

1. Since the error curves for these large dispersions stay reasonably close to nominal and have a similiar shape to the nominal (i.e., go up when the nominal goes up and down when the nominal goes down), it can be concluded that monitoring attitude errors is feasible, i.e., reasonable (expected or 3σ) dispersions will follow the nominal very well and, hopefully, catastrophic failures will thus be detectable.

2. Since the powered flight paths for the dispersed cases here are considerably different from the nominal one, it can be concluded that the initial DAP effects will not appreciably hurt the attitude error curves (nothing can be said for the DAP effects on total attitudes at this time).

3. As on figure 8(b), these curves imply that any known dispersions (e.g., thrust) should be compensated for in the spacecraft targeting if possible.

The author presently has no explanation for the behavior of the Mission G high thrust curve (curve a) for the first 40 seconds. At this stage of the game, nothing further is being done to explain it. It will be written off as just a characteristic of this bad a dispersion unless it shows up in later TLI monitoring data.

Figure 18(b) - Inertial yaw error history for constant thrust and specific impulse dispersions for Missions E and G.- The comments about figure 14(b) apply here. The author presently has no explanation for the behavior of the Mission G low thrust curve's (curve b) behavior during the first 80 seconds of the burn. Again, no explanation is presently being pursued.

Figure 19 - Inertial pitch rate history for dispersed ignition states for Missions E and G.- Note that curve 3 is initially negative when the nominal was positive. This means that if there is to be this kind of difference in pitch rate due to state vector, the crew must be informed of this so that they will not take some sort of corrective action. It should be fairly easy to determine if this will happen, but if it cannot be for some reason, this parameter should be ignored initially.

Figure 21 - Inertial pitch rate history for the two thrust and specific impulse models in Mission G.- No Mission E pitch rates using the models are given because, as mentioned in the comments on figure 14, the data did not seem reasonable. The bumps on the Mission G curves are due to the periodic thrust fluctuations.

Figure 22 - Inertial yaw rate history for an out-of-plane position dispersion of the ignition state in Mission E.- A yaw rate of 0.18 deg/sec for 150 seconds gives about 27°, agreeing with figure 16.

CONCLUSIONS

The following conclusions should be viewed in light of the assumptions made to generate the data. They are the conclusions suggested by this data only; final confirmation of the feasibility of monitoring TLI should come from a six-dimensional vehicle simulation. Consequently it is recommended that more sophisticated studies than done here be undertaken to check the feasibility of TLI monitoring.

1. Attitude histories can only be used as gross monitoring parameters. This also applies to attitude rate histories.

2. Attitude error histories may be more accurate to monitor than the total attitudes or attitude rates. The data in this note only indicates this may be so; it does not prove it. However, it can be concluded from the data that attitude error monitoring will be meaningful.

3. It is unnecessary to correct for small EPO errors since the possible thrust dispersions should swamp these errors. However, it is recommended that this be done as a standard procedure (i.e., the CMC be targeted as near as possible to the hypersurface defined outgoing conic orbit). Reference 4, flow chart 1, shows that the CMC targeting updates will account for any known dispersions.

4. Although impulsive targeting for CMC control of Mission E TLI comes very close to the desired end conditions, it is not best for monitoring. Since the attitude errors for this targeting show a divergence much farther from the end of the burn than IGMBO targeting, it is feared that this divergence will start even further from the end of the burn in real life.

5. V_g is not an effective parameter to monitor. The time-to-go should be sufficient.

6. The 1-second sampling rate on α_{TS} will have negligible effect on monitoring.

7. The behavior of the attitude error histories due to the constant thrust and specific impulse errors indicates that the DAP effects will be of little consequence in attitude error monitoring. No conclusion about the DAP effects on the total attitudes and rates can be drawn here.

8. Because of the possible problem due to different state vectors in the CMC and Saturn computer, any state vector updates should provide the same vectors to both the CMC and Saturn.

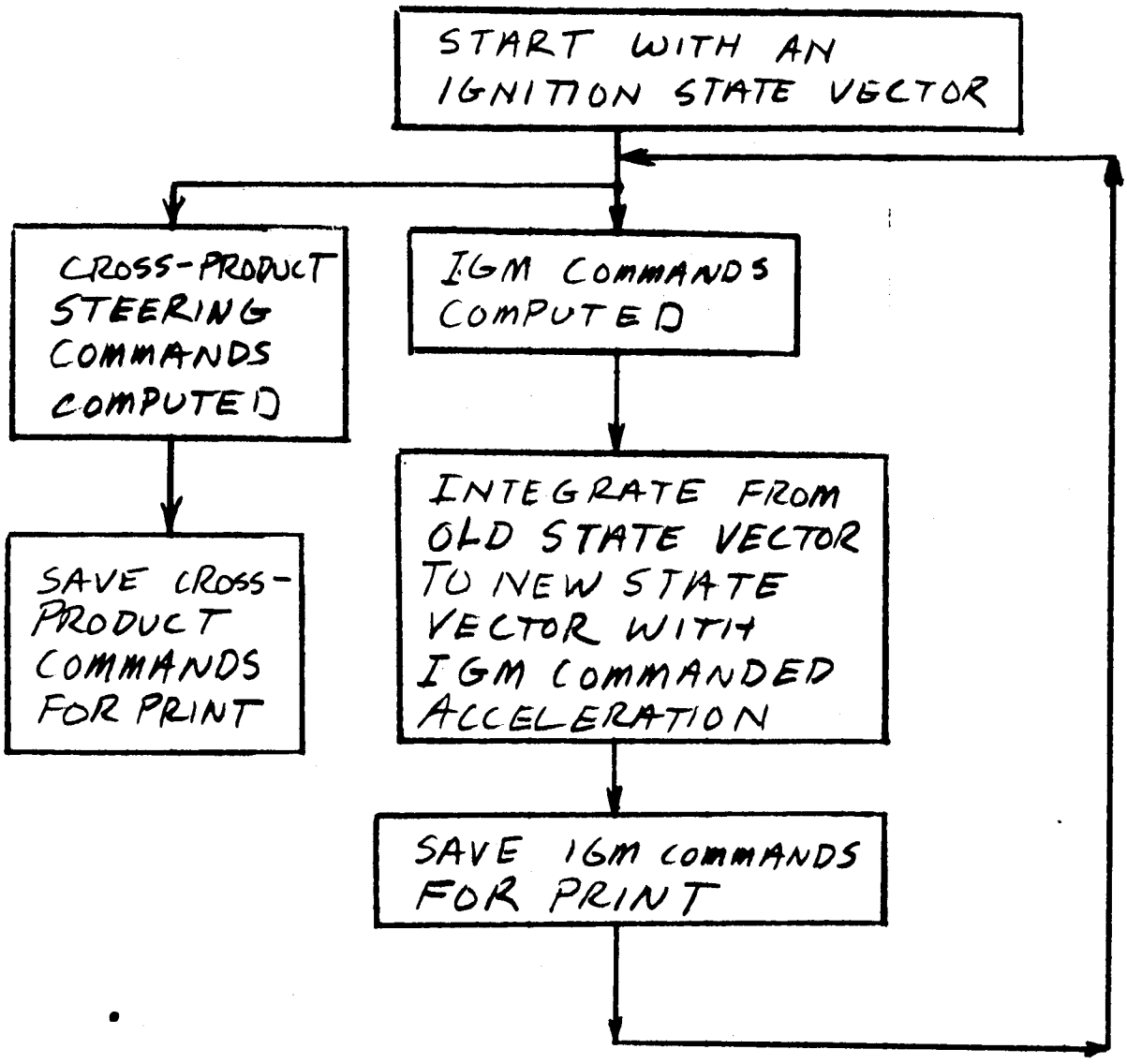

FUNCTIONAL FLOW TO COMPUTE THE CROSS-PRODUCT STEERING COMMANDED ATTITUDES AND V_g

TABLE I.- DISPERSIONS CONSIDERED FOR MISSION G

	Ignition State	
1.	+1.0 n. mi., +10.0 fps	an increase of 1.0 n. mi. in each geocentric position component magnitude and 10.0 fps in each geocentric velocity component magnitude
2.	-1.0 n. mi., -10.0 fps	a decrease of 1.0 n. mi. in each geocentric position component magnitude and 10.0 fps in each geocentric velocity component magnitude
	Ignition Time	
1.	3-second ignition delay	ignition occurs 3 seconds past the nominal ignition time in the nominal EPO
	Thrust and Specific Impulse	
1.	High thrust, low specific impulse models	thrust model with initial thrust increase and specific impulse model with initial specific impulse decrease
2.	Low thrust, high specific impulse models	thrust model with initial thrust decrease and specific impulse model with initial specific impulse increase
3.	High thrust, low specific impulse	+30 000-lb thrust and -4 seconds specific impulse
4.	Low thrust, high specific impulse	-30 000-lb thrust and +4 seconds specific impulse

TABLE II.- DISPERSIONS CONSIDERED FOR MISSION E

[Plumbline System]

Ignition State

Inertial geocentric state	Nominal	+.5 km, +.001[a] km/sec	+10 km out of plane[b]	+.01 km/sec[c]
X, n. mi.	144.4365	144.6306	146.2311	144.4365
Y, n. mi.	3152.1841	3152.6090	3154.5529	3152.1841
Z, n. mi.	1620.2525	1620.2297	1615.7444	1620.2525
$\dot{X}$, fps	-24048.951	-24052.048	-24048.951	-24079.928
$\dot{Y}$, fps	4856.4720	4859.7883	4856.4720	4889.6350
$\dot{Z}$, fps	-7286.4599	-7289.8800	-7286.4599	-7320.6613

Thrust and Specific Impulse

1.	High thrust, low specific impulse	+30 000-lb thrust and -2.8 seconds specific impulse
2.	Low thrust, high specific impulse	-30 000-lb thrust and +3.3 seconds specific impulse

[a] +.5 km, +.001 km/sec = an increase of .5 km in each plumbline position component magnitude and .001 km/sec in each plumbline velocity component magnitude.

[b] +10 km out of plane = an increase of 10 km in the out-of-plane plumbline component magnitude.

[c] +.01 km/sec = an increase of .01 km/sec in each plumbline velocity component magnitude.

TABLE III.- α_{TS} AND THE WEDGE ANGLE BETWEEN THE NOMINAL AND DISPERSED EPO'S FOR THE IGNITION STATE DISPERSIONS

Mission E

Dispersion	α_{TS}	Wedge angle
Nominal	29.660440	0.0000
+5 km +.001 km/sec	29.719837	0.0839
+10.0 km out of plane	29.681201	0.1744
+.01 km/sec	29.660436	0.1097

Mission G

Nominal	9.89575	0.0000
+1.0 n. mi. +10.0 fps	9.89717	0.1562
-1.0 n. mi. -10.0 fps	9.89434	0.1477

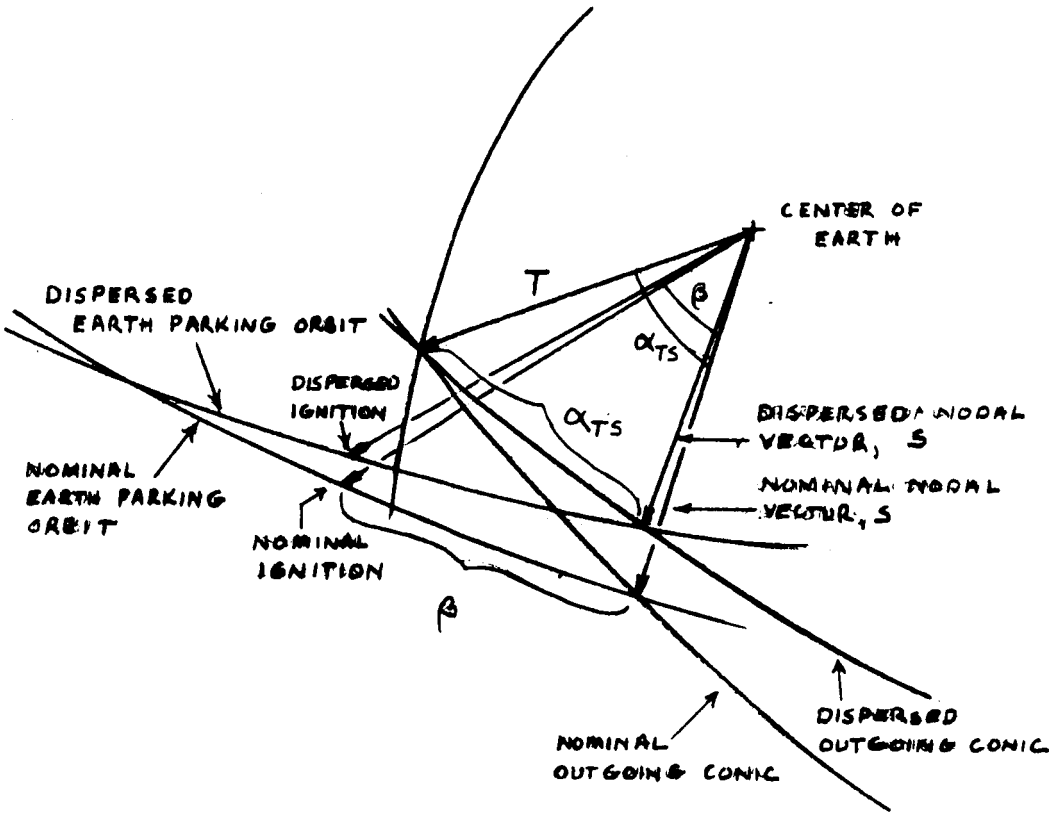

FIGURE 1.
RESTART GEOMETRY.

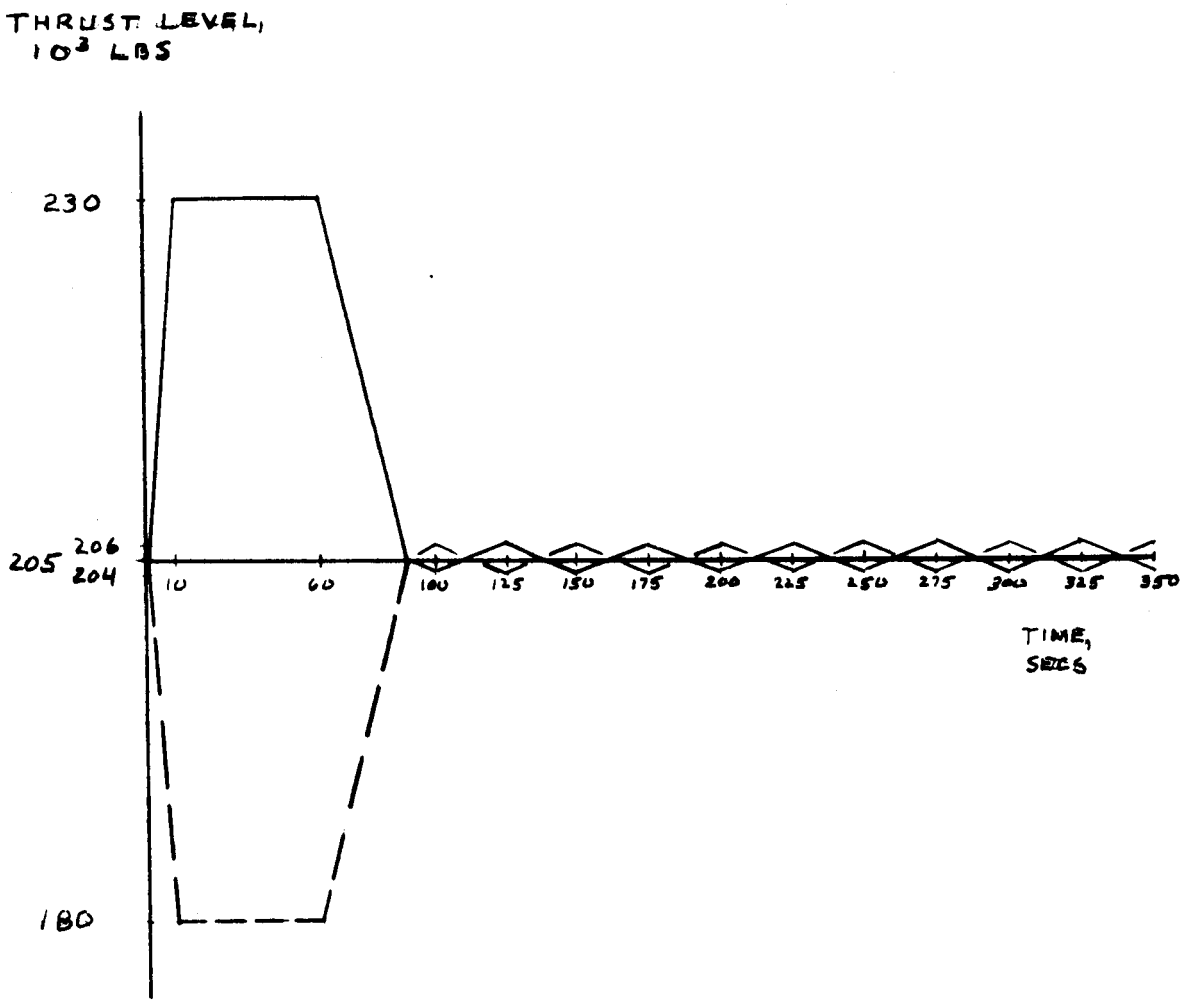

FIGURE 2.
THRUST MODEL.

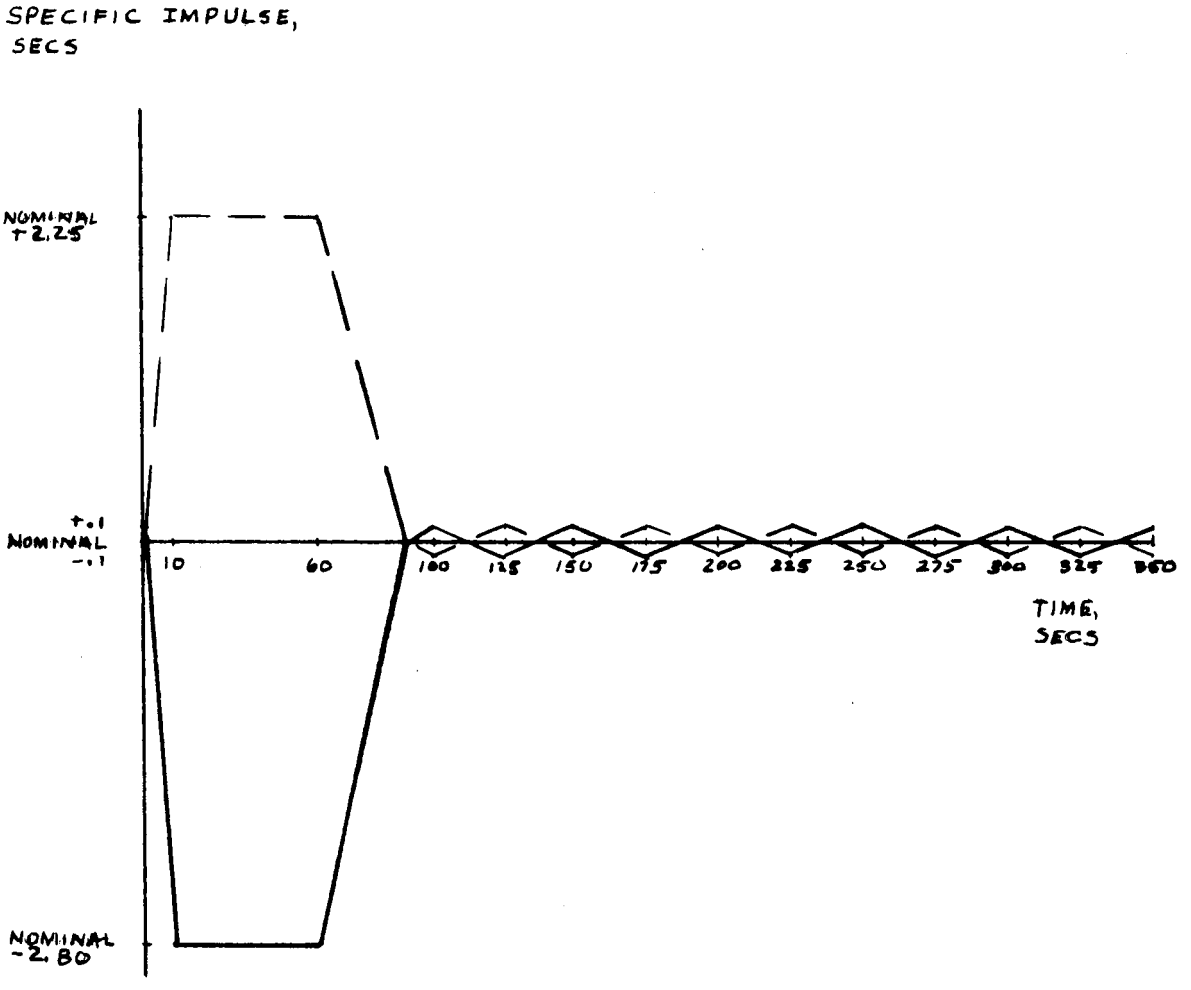

FIGURE 3.—
SPECIFIC IMPULSE MODEL.

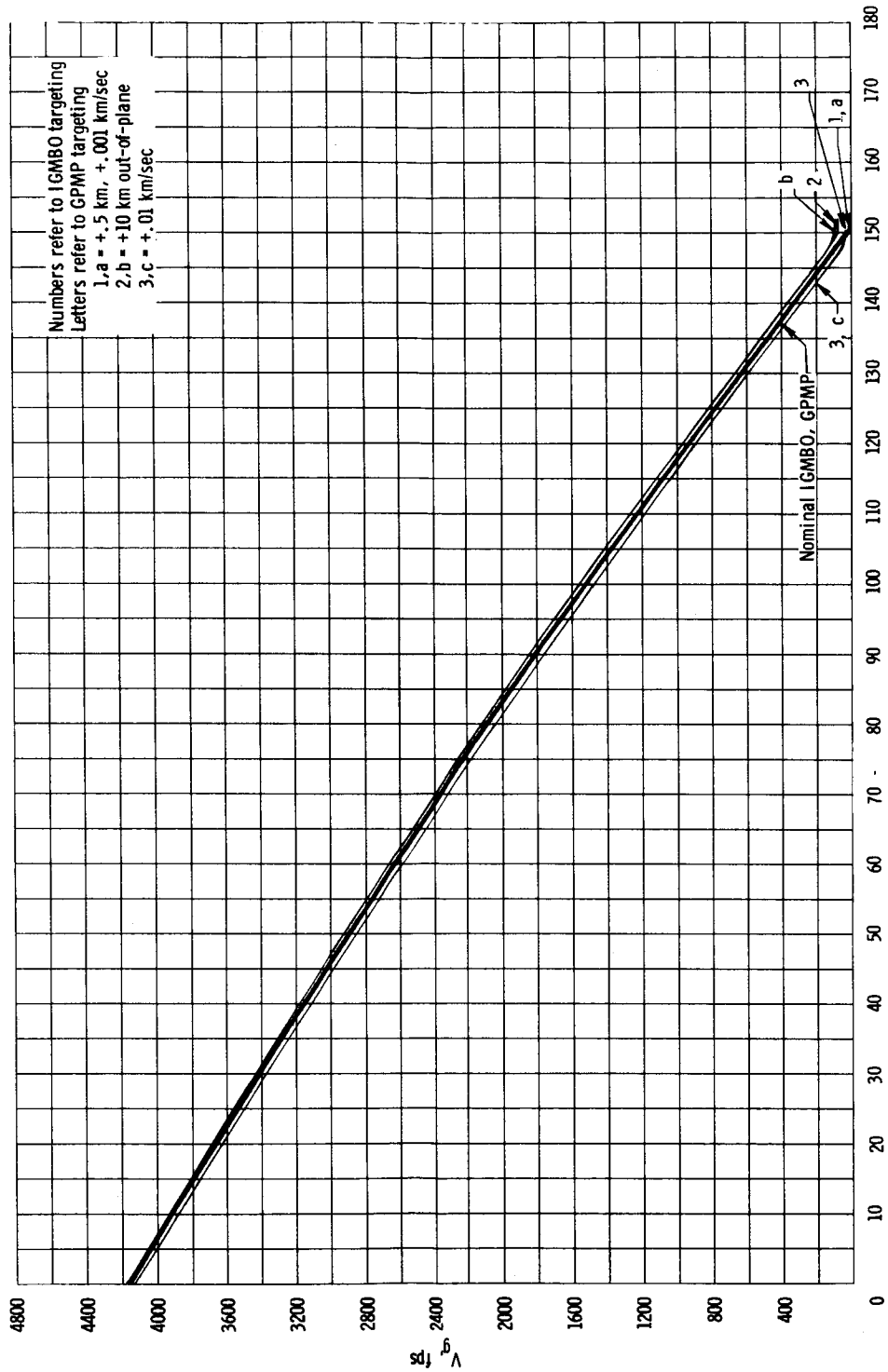

Figure 4.- V_g history for dispersed ignition states for the two Mission E targeting schemes.

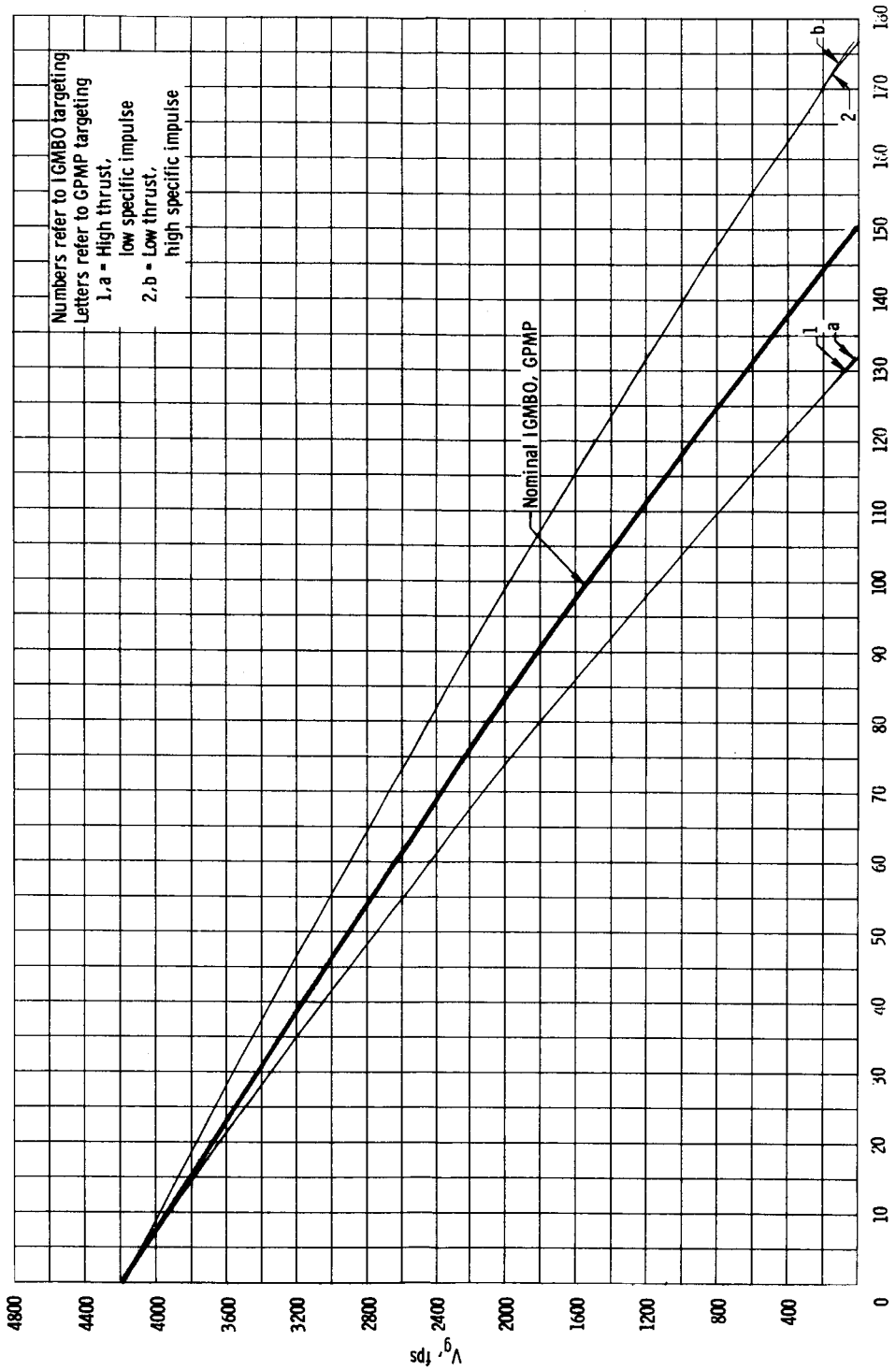

Figure 5.- V_g history for constant thrust and specific impulse dispersions for the two Mission E targeting schemes.

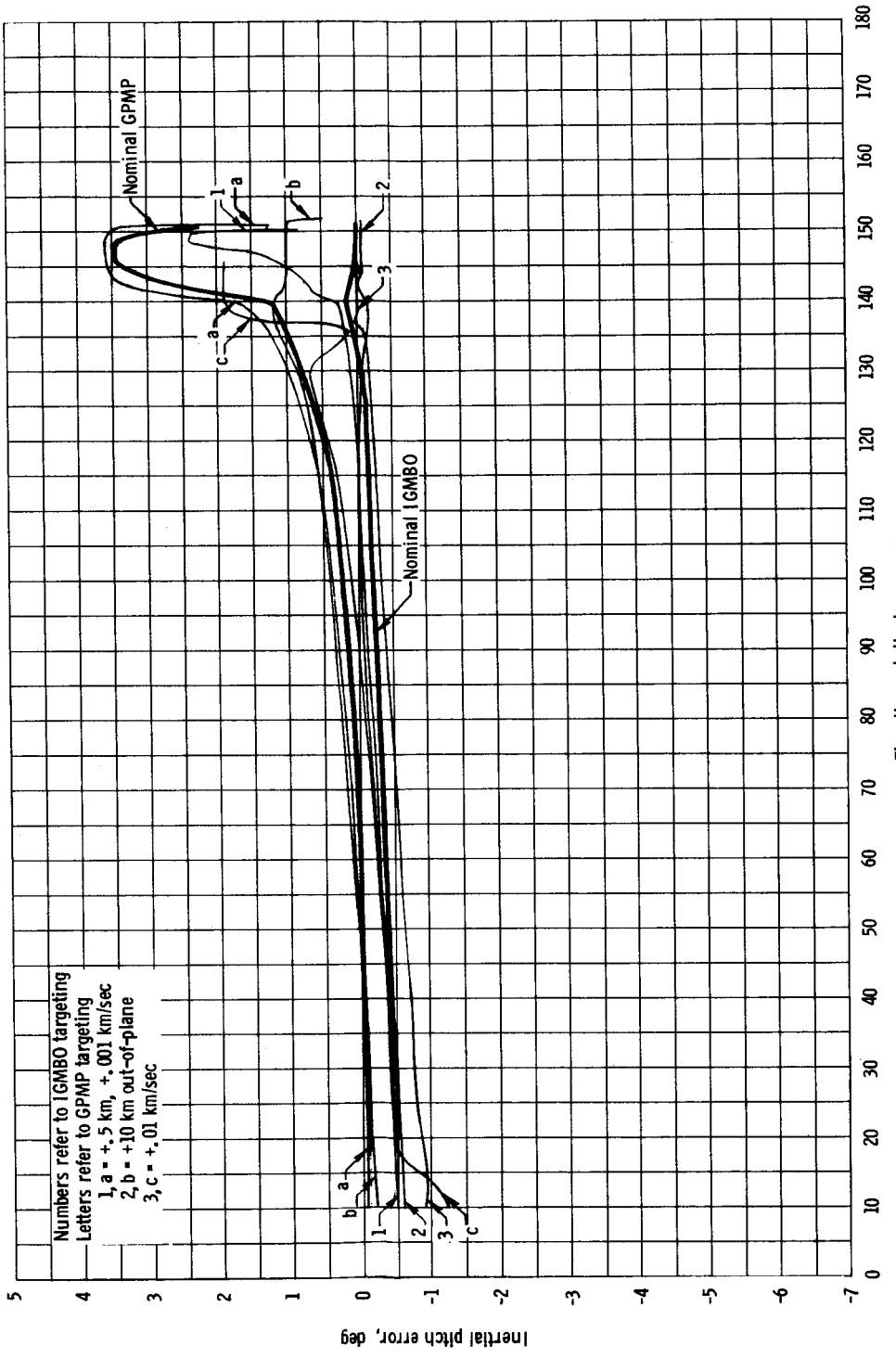

Figure 6.- Inertial pitch error history for dispersed ignition states for the two Mission E targeting schemes.

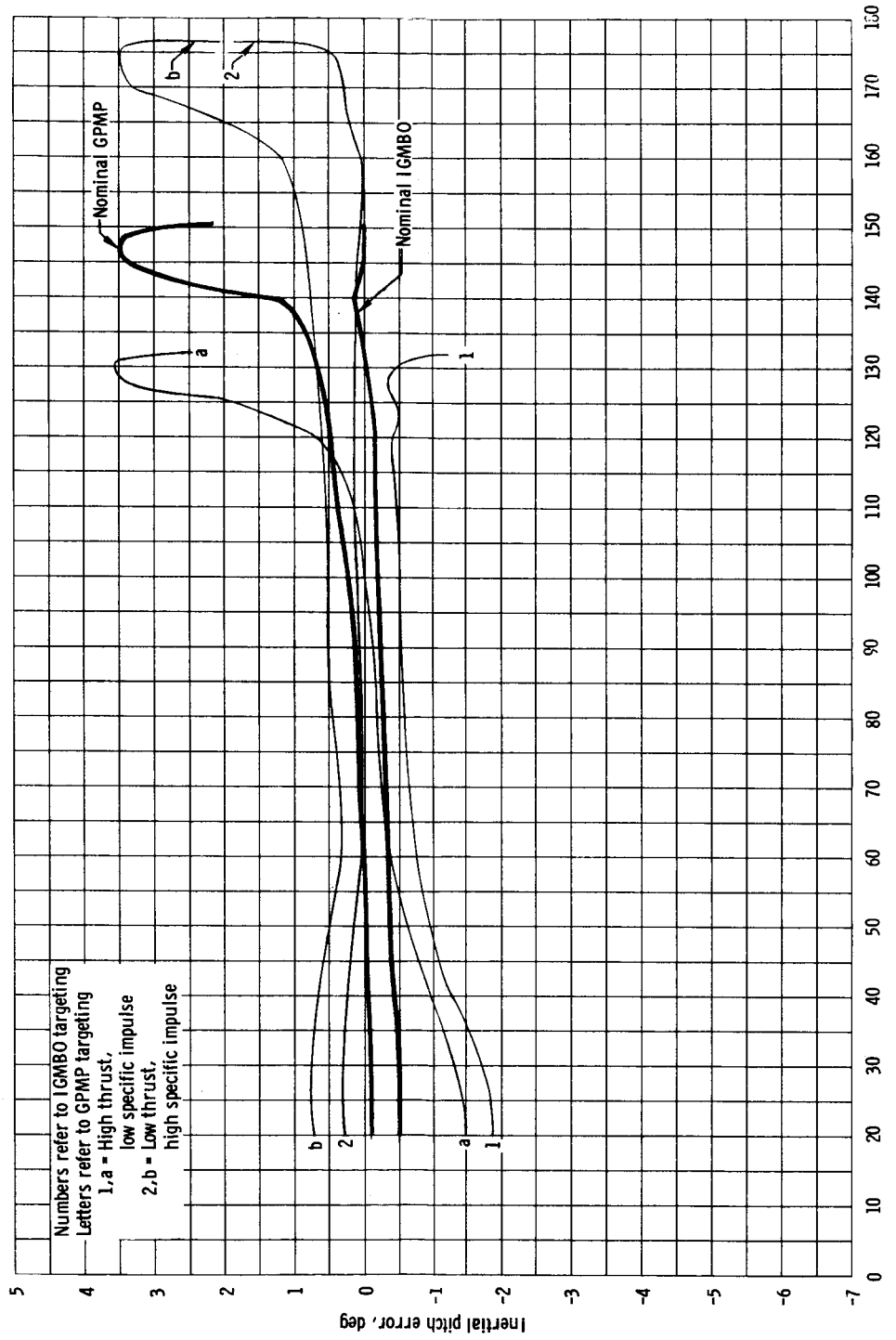

Figure 7.- Inertial pitch error history for constant thrust and specific impulse dispersions for the two Mission E targeting schemes.

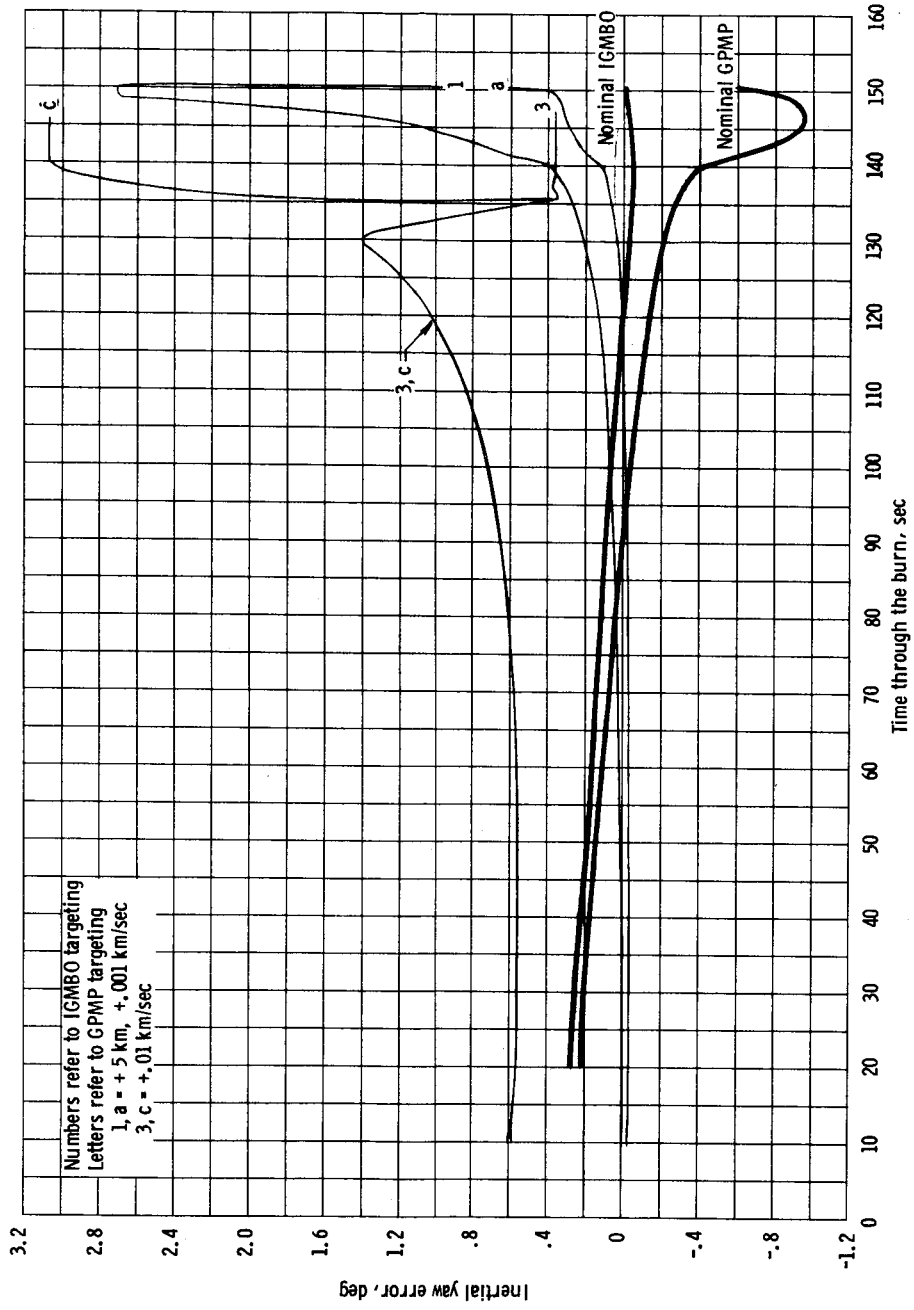

(a) Dispersed ignition states.

Figure 8.- Inertial yaw error history for the two Mission E targeting schemes.

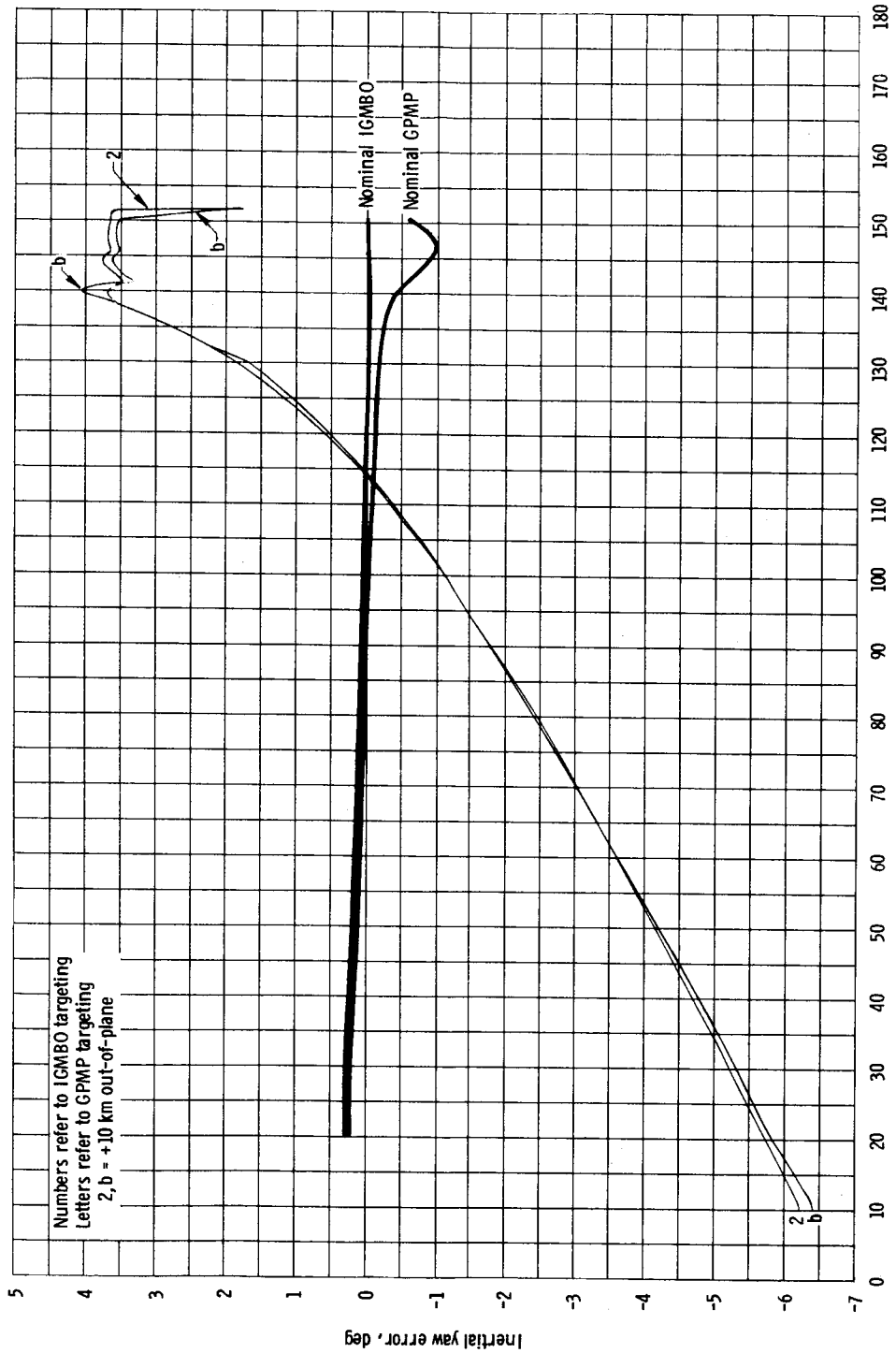

(b) Out-of-plane position dispersion in the ignition state.

Figure 8. - Concluded.

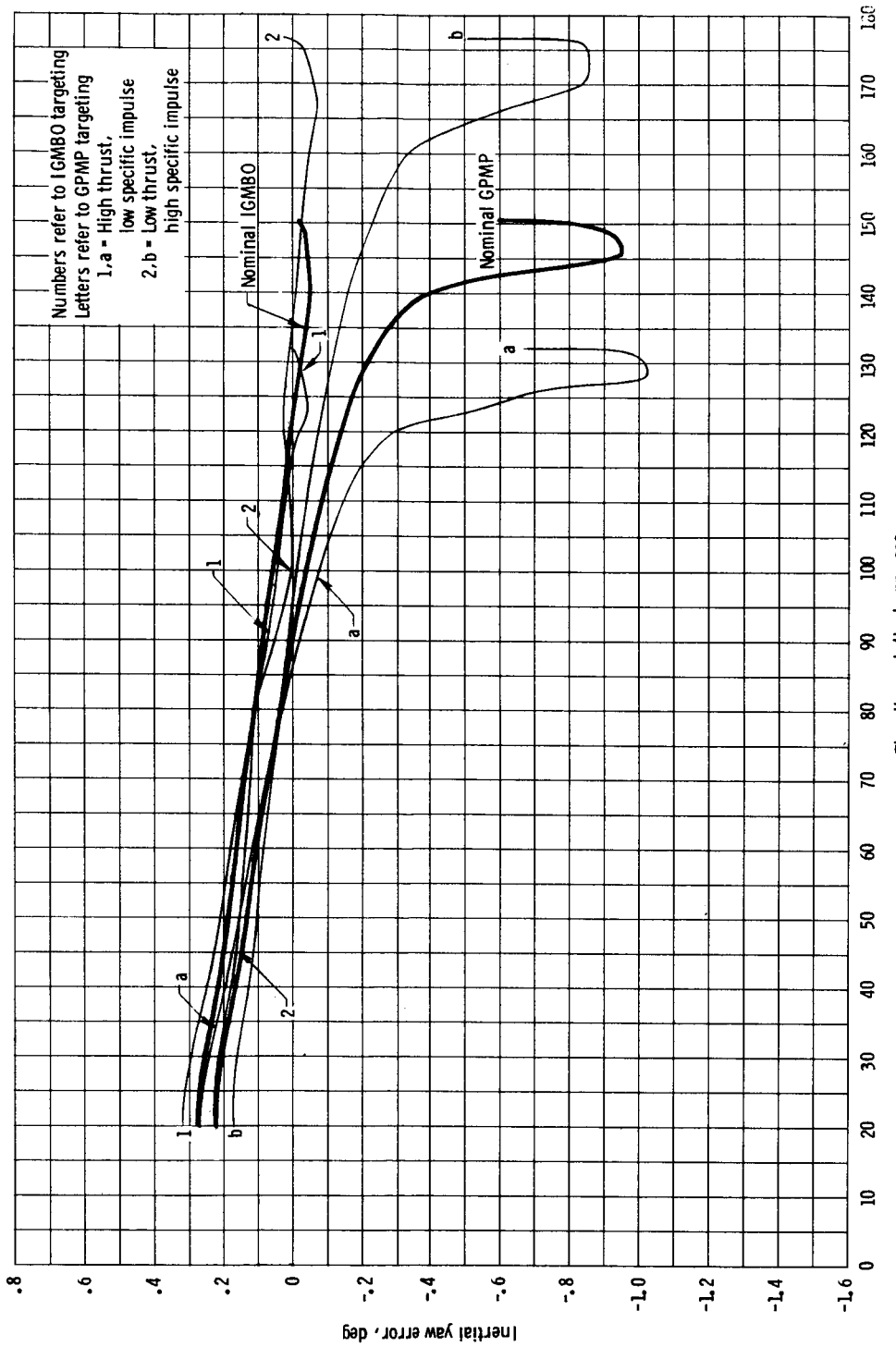

Figure 9.- Inertial yaw error history for constant thrust and specific impulse dispersions for the two Mission E targeting schemes.

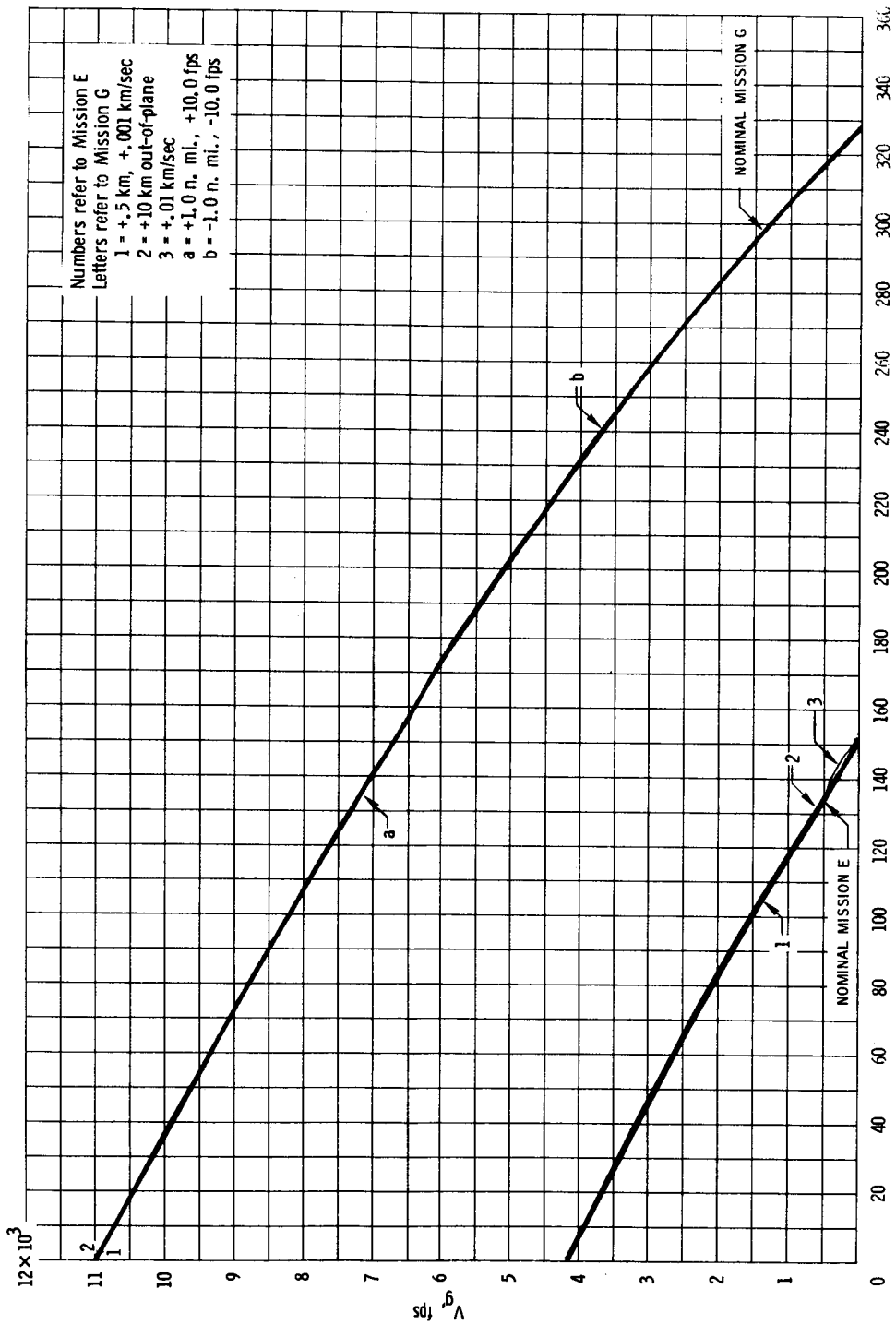

Figure 10. - V_g history for dispersed ignition states for Missions E and G.

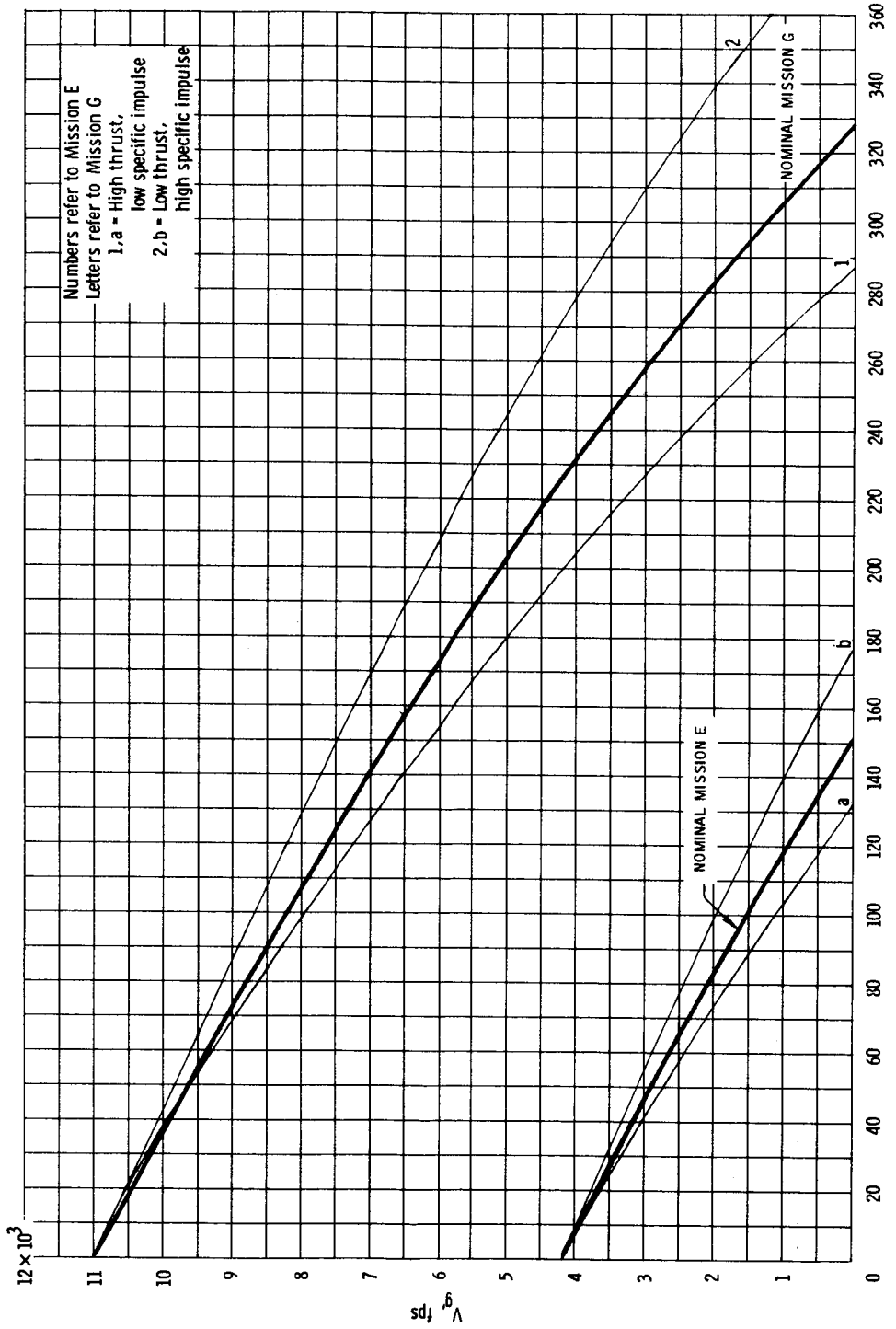

Figure 11. - V_g history for constant thrust and specific impulse dispersions for Missions E and G.

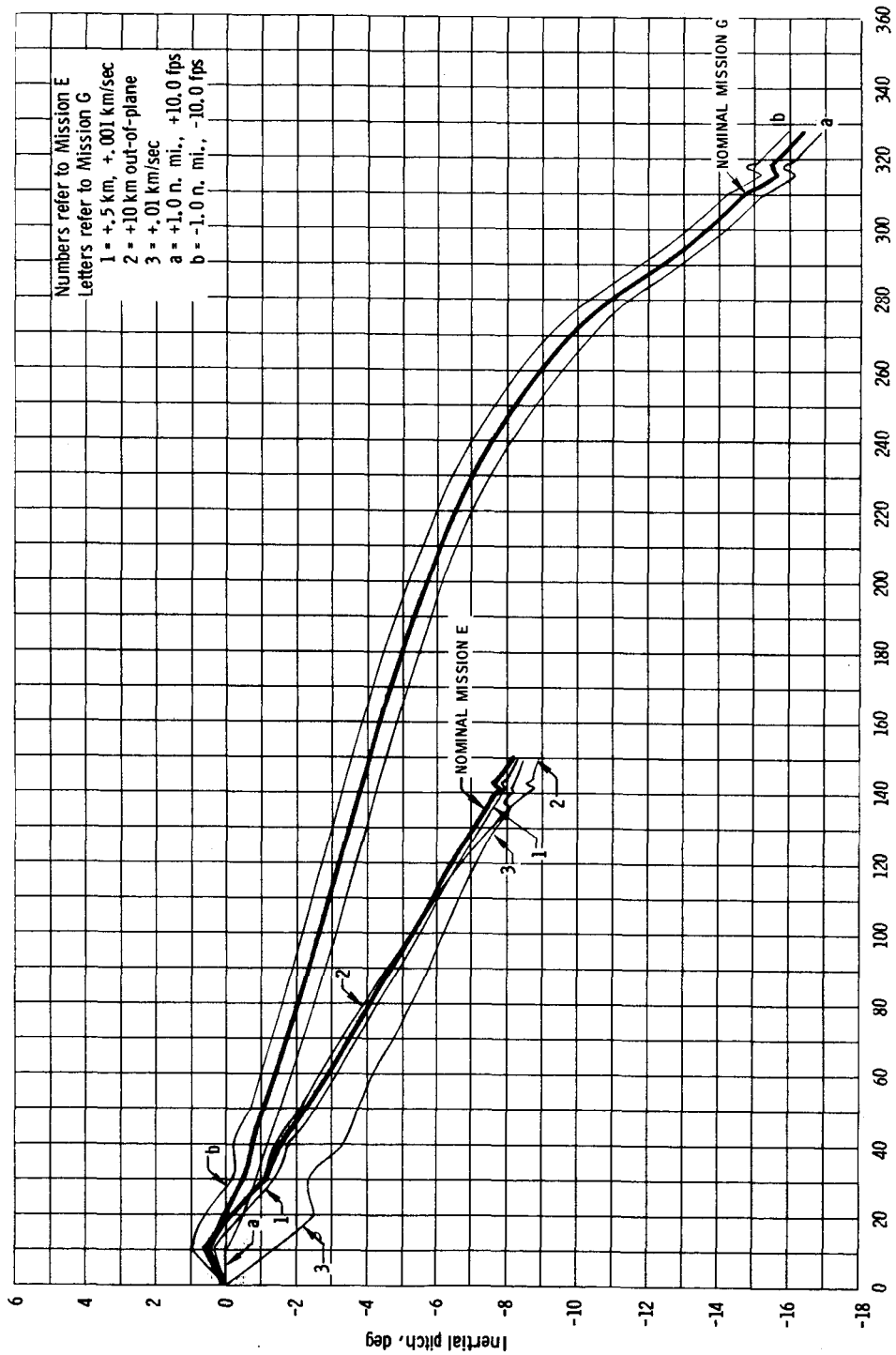

(a) Pitch.

Figure 12 - Inertial pitch and pitch error histories for dispersed ignition states for Missions E and G.

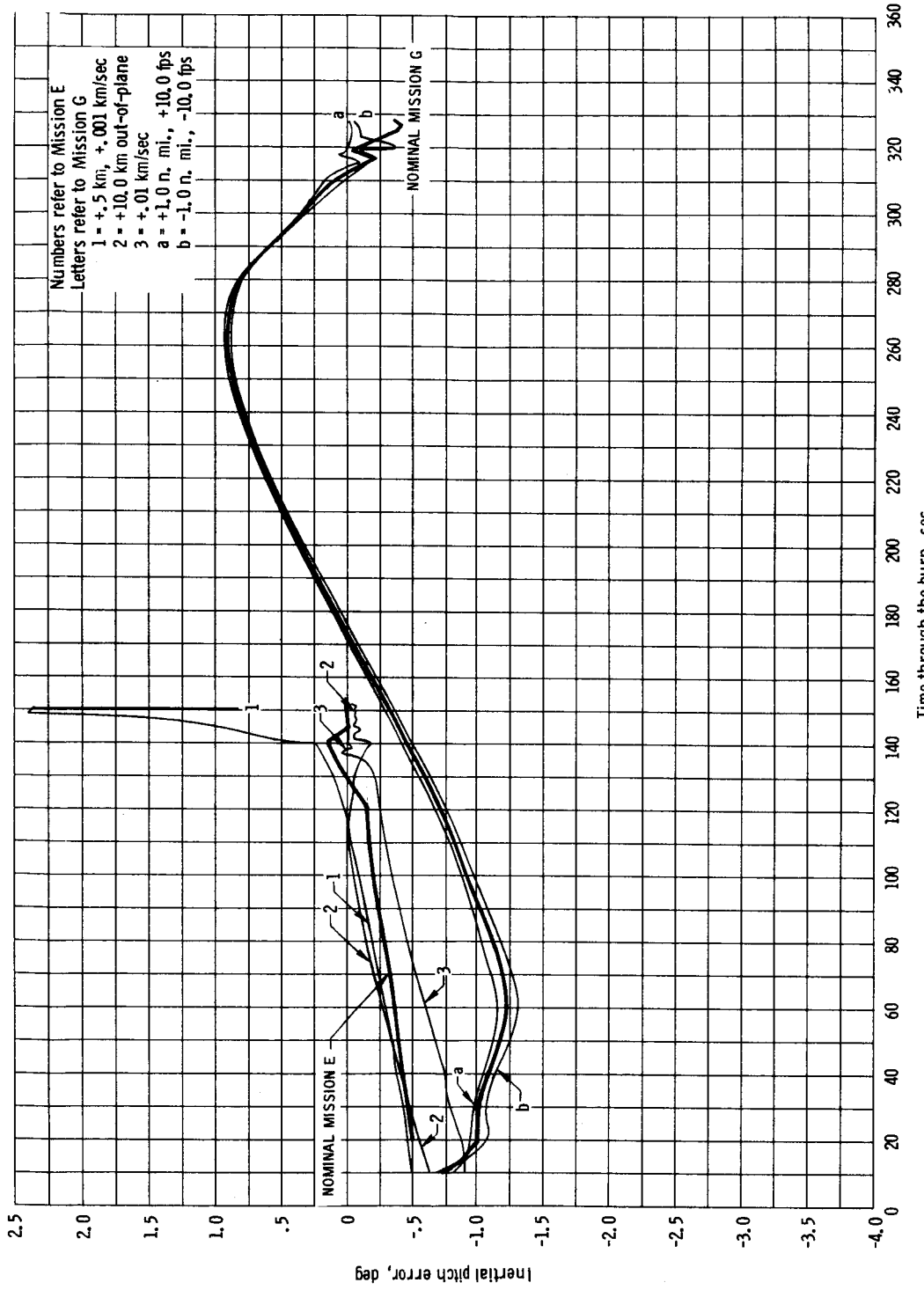

(b) Pitch error.

Figure 12. - Concluded.

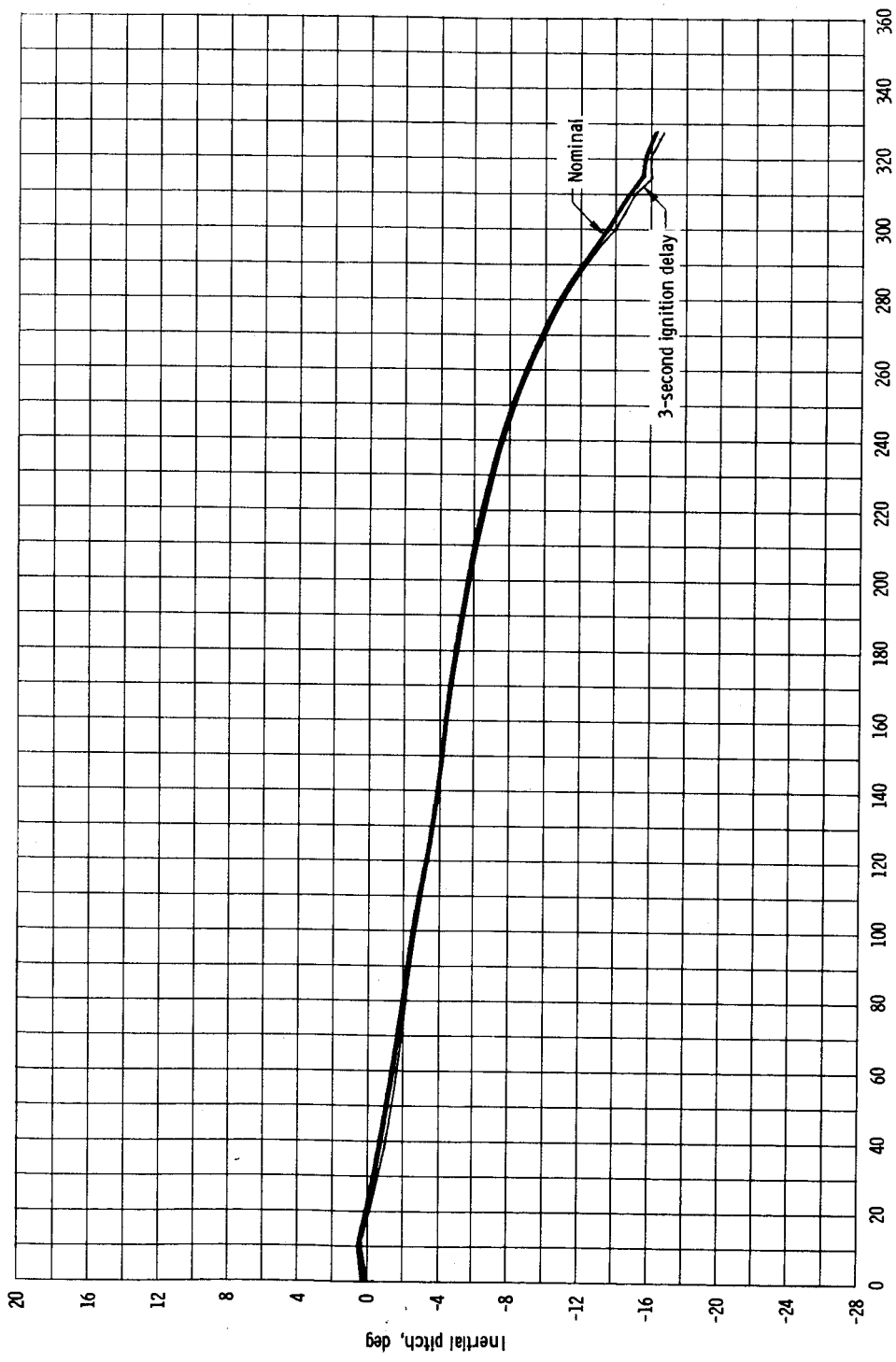

(a) Pitch.

Figure 13.- Inertial pitch and pitch error histories for a 3-second ignition delay in Mission G.

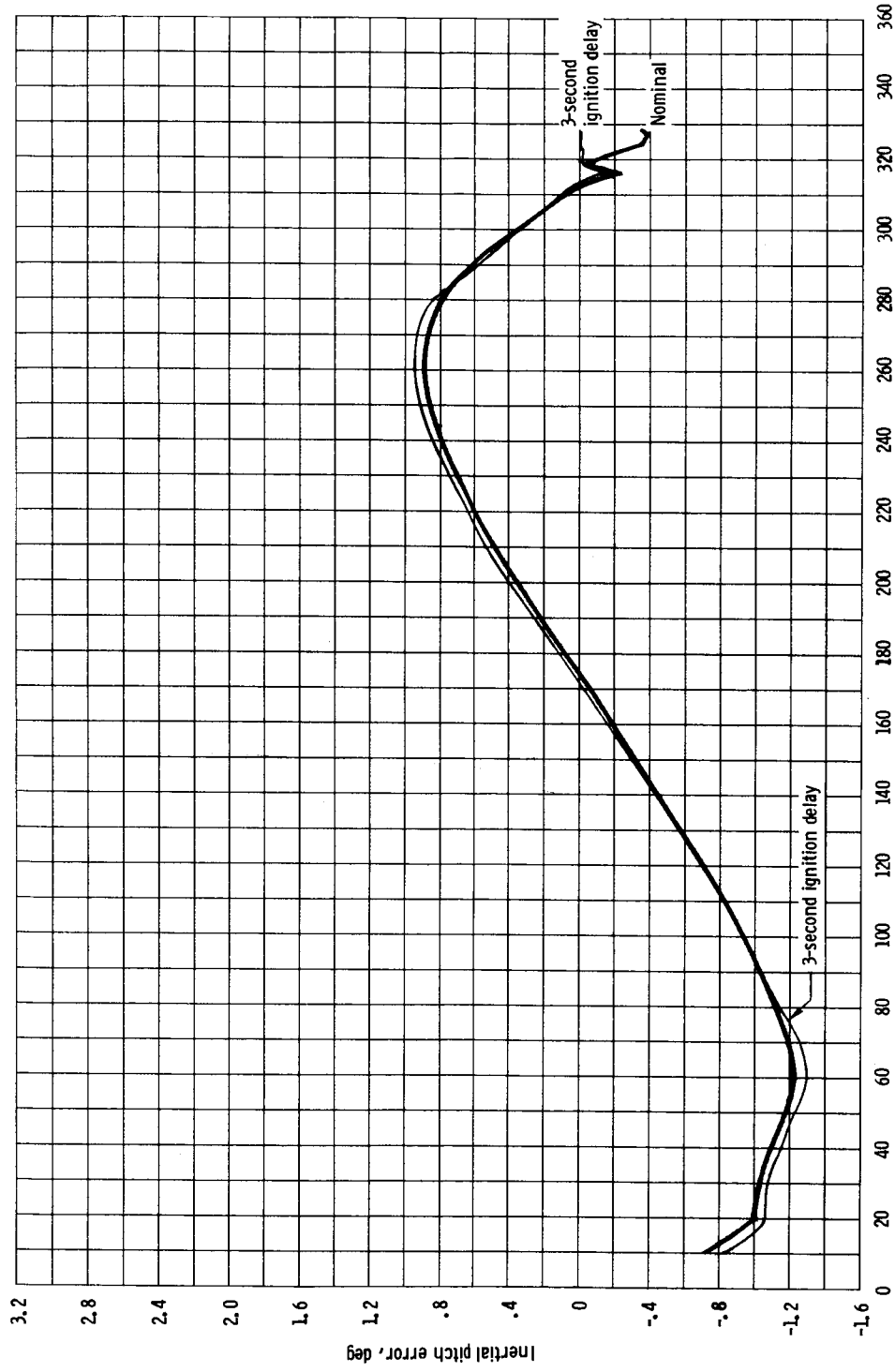

(b) Pitch error.

Figure 13. - Concluded.

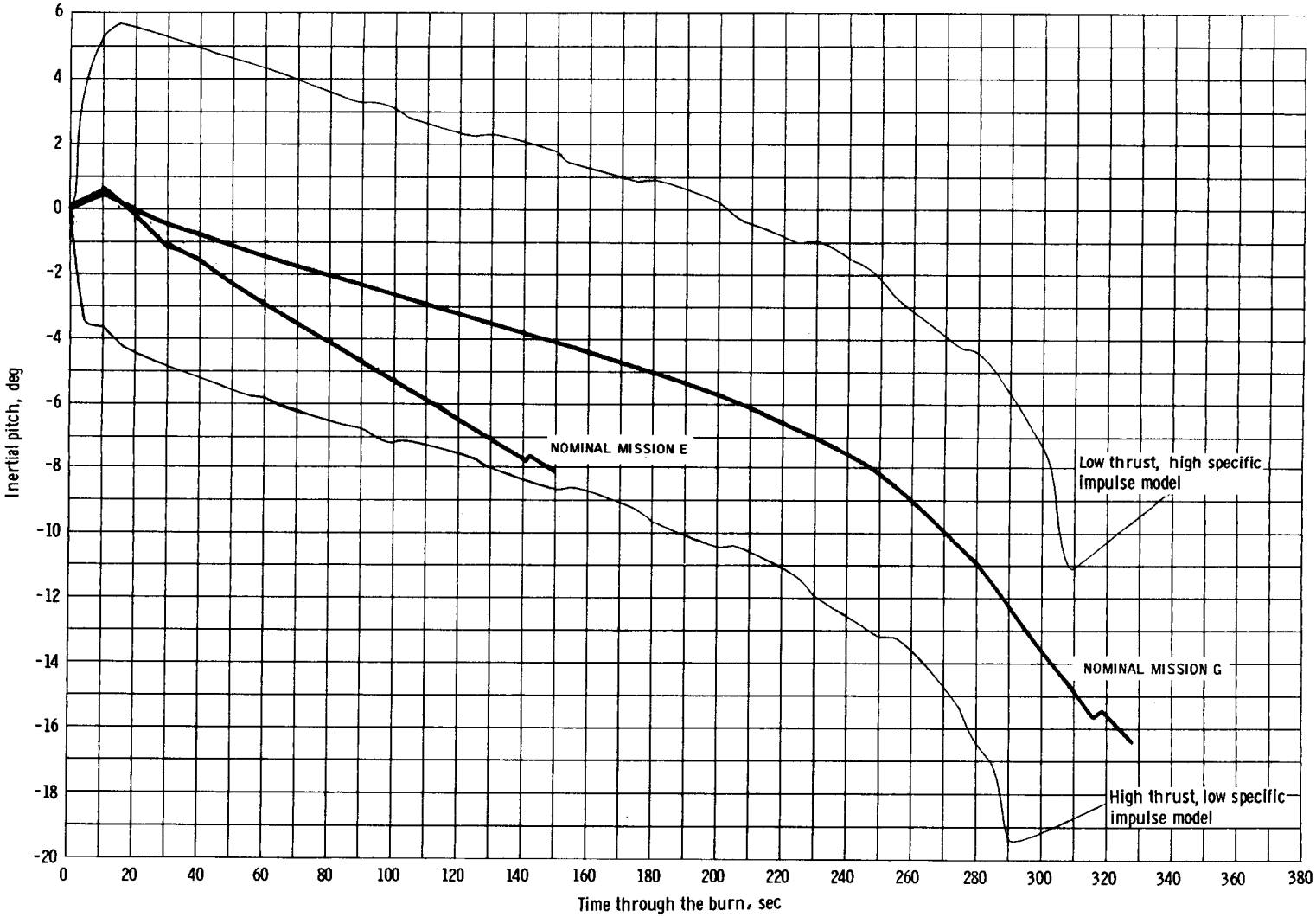

(a) Pitch for the two thrust and specific impulse models in Mission G.

Figure 14. - Inertial pitch and pitch error histories.

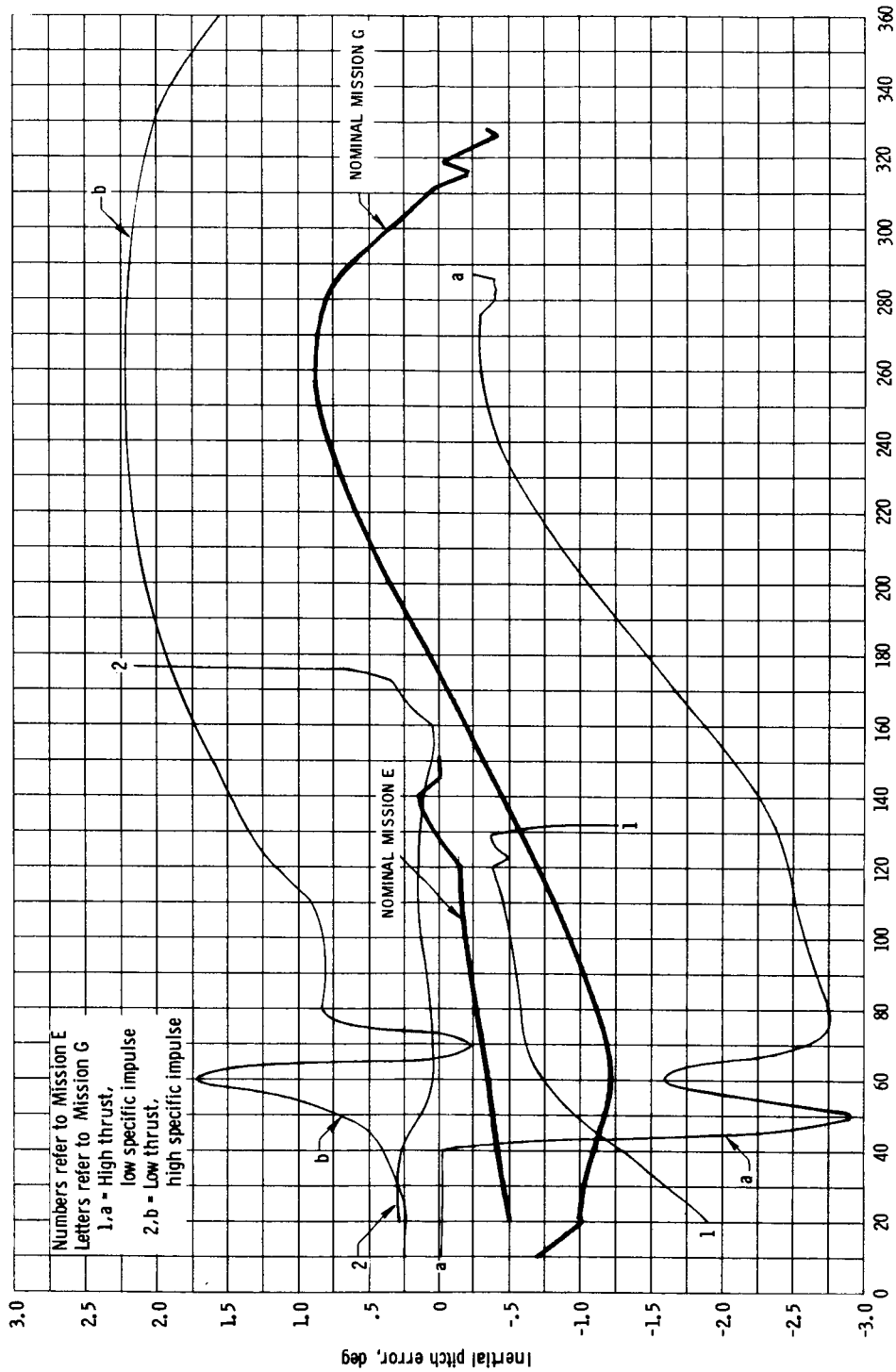

(b) Pitch error for constant thrust and specific impulse dispersion in Missions E and G.

Figure 14. - Concluded.

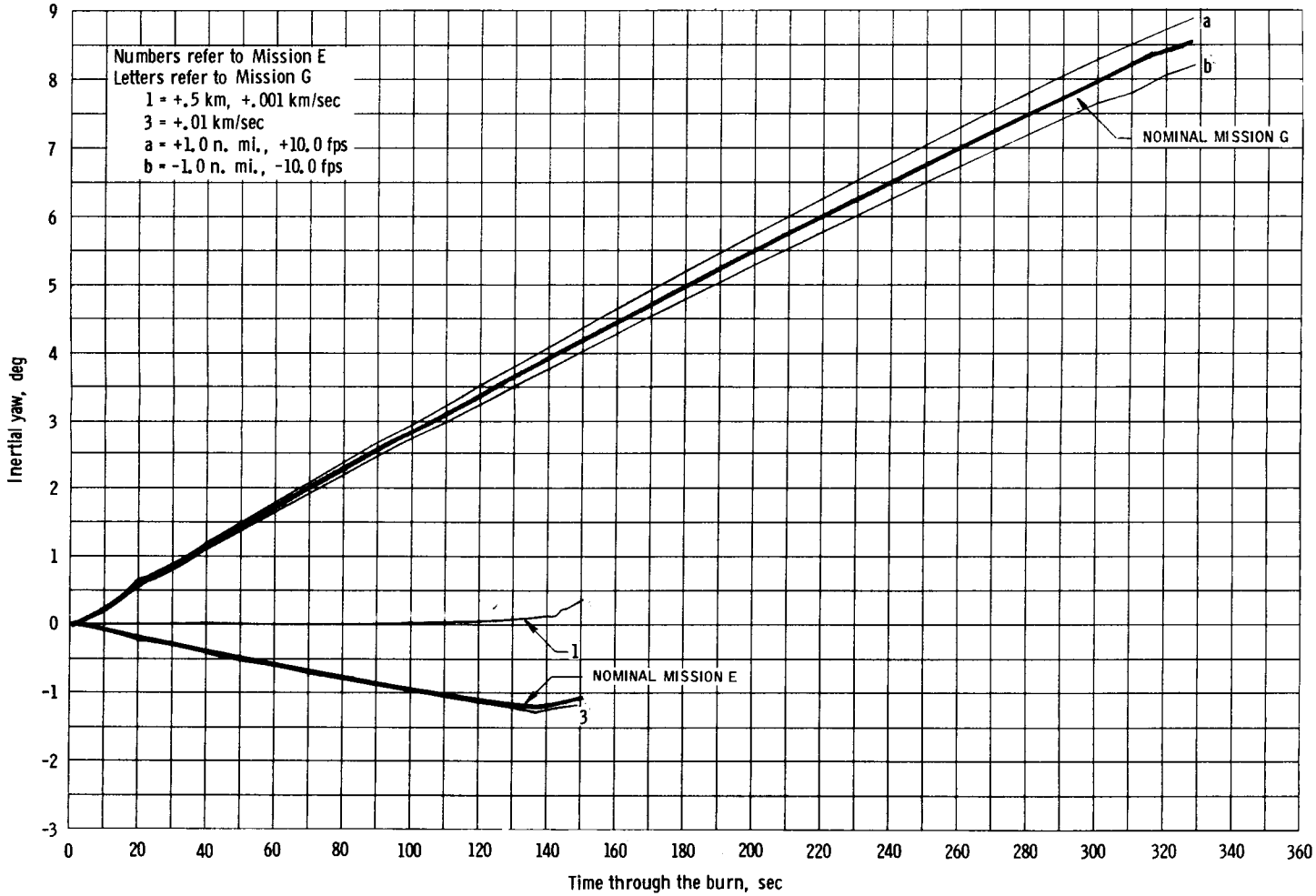

(a) Yaw.

Figure 15. - Inertial yaw and yaw error histories for dispersed ignition states for Missions E and G.

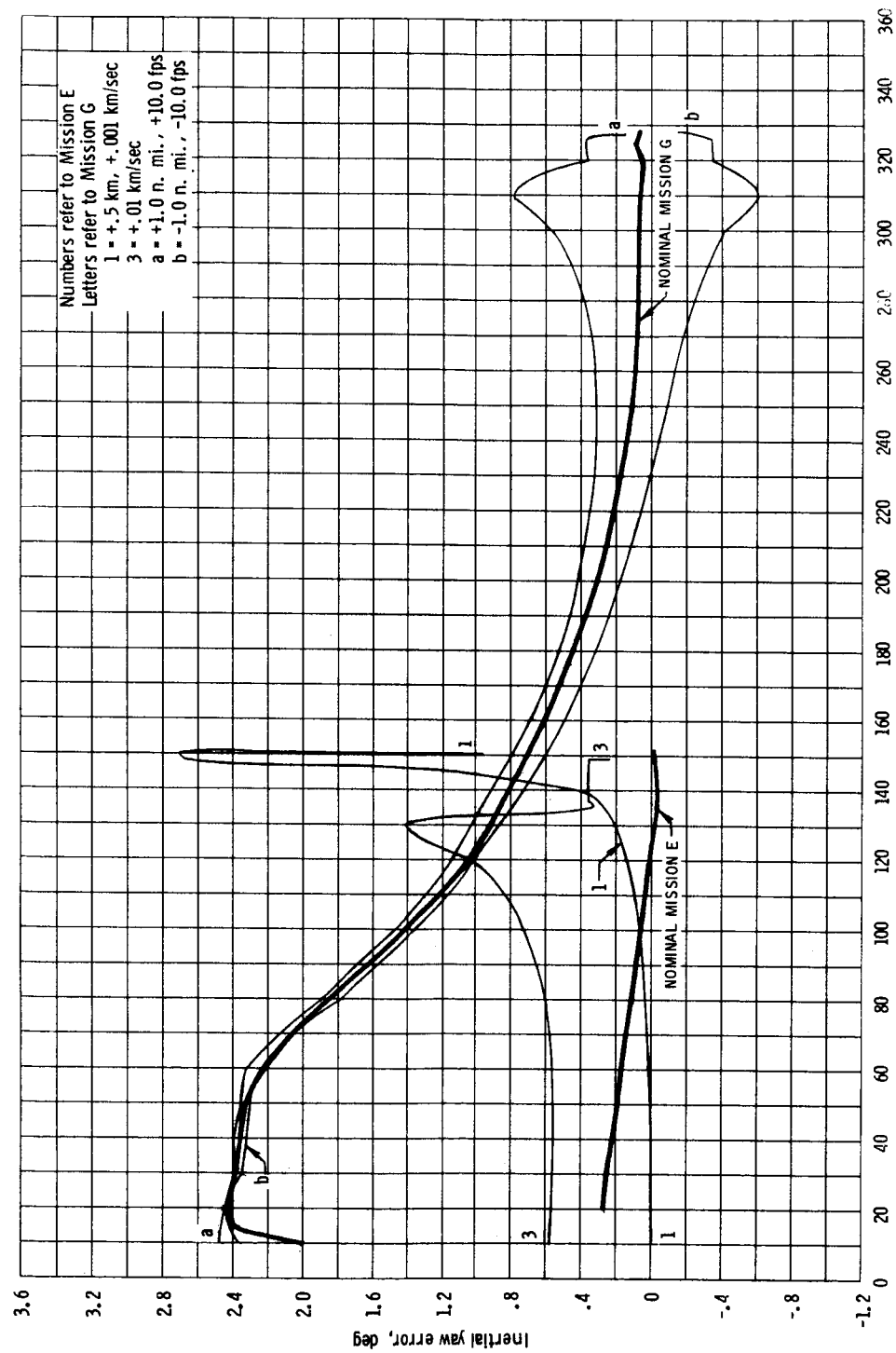

(b) Yaw error.

Figure 15. - Concluded.

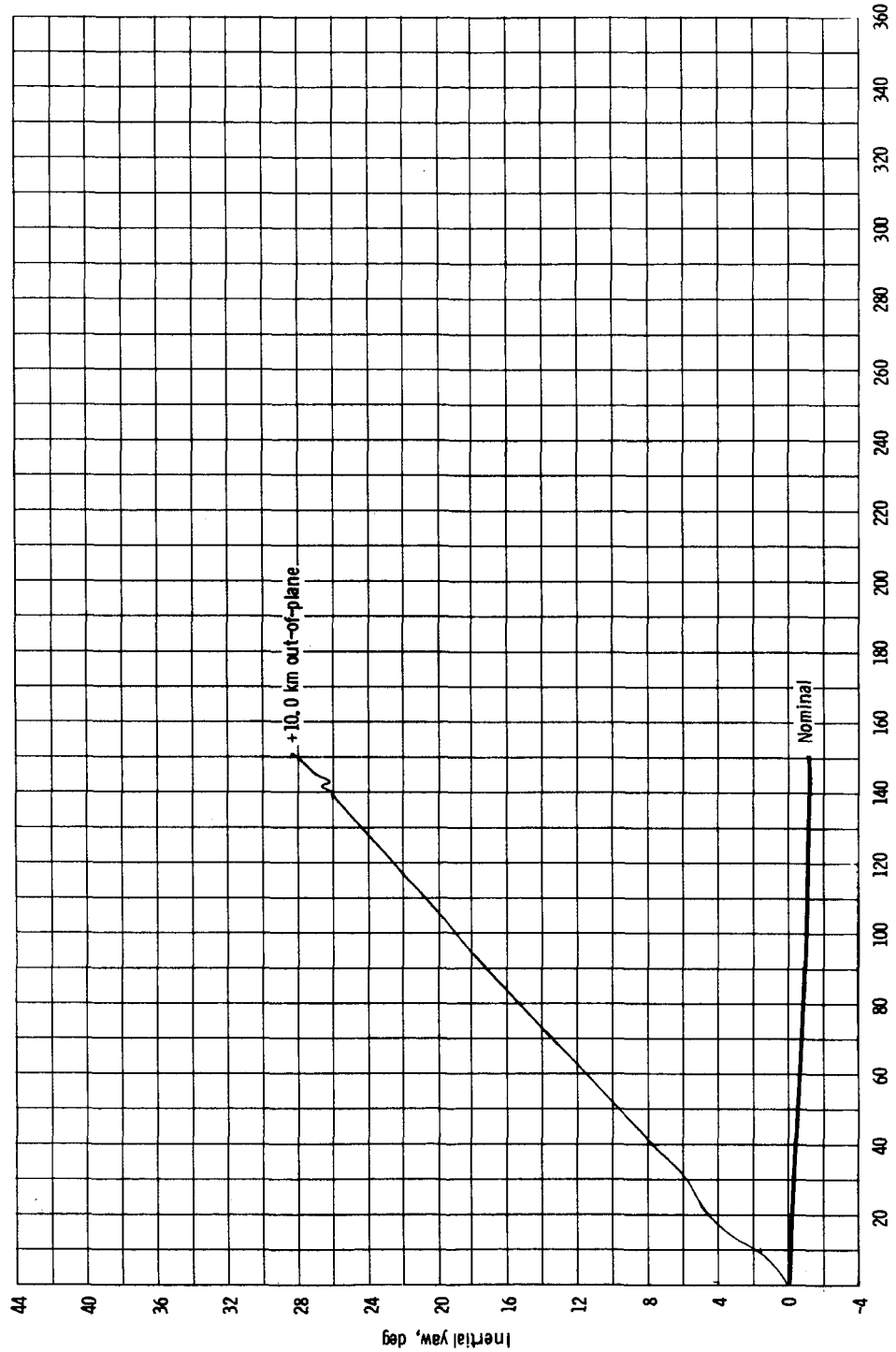

(a) Yaw.

Figure 16.- Inertial yaw and yaw error histories for an out-of-plane position dispersion of the ignition state in Mission E.

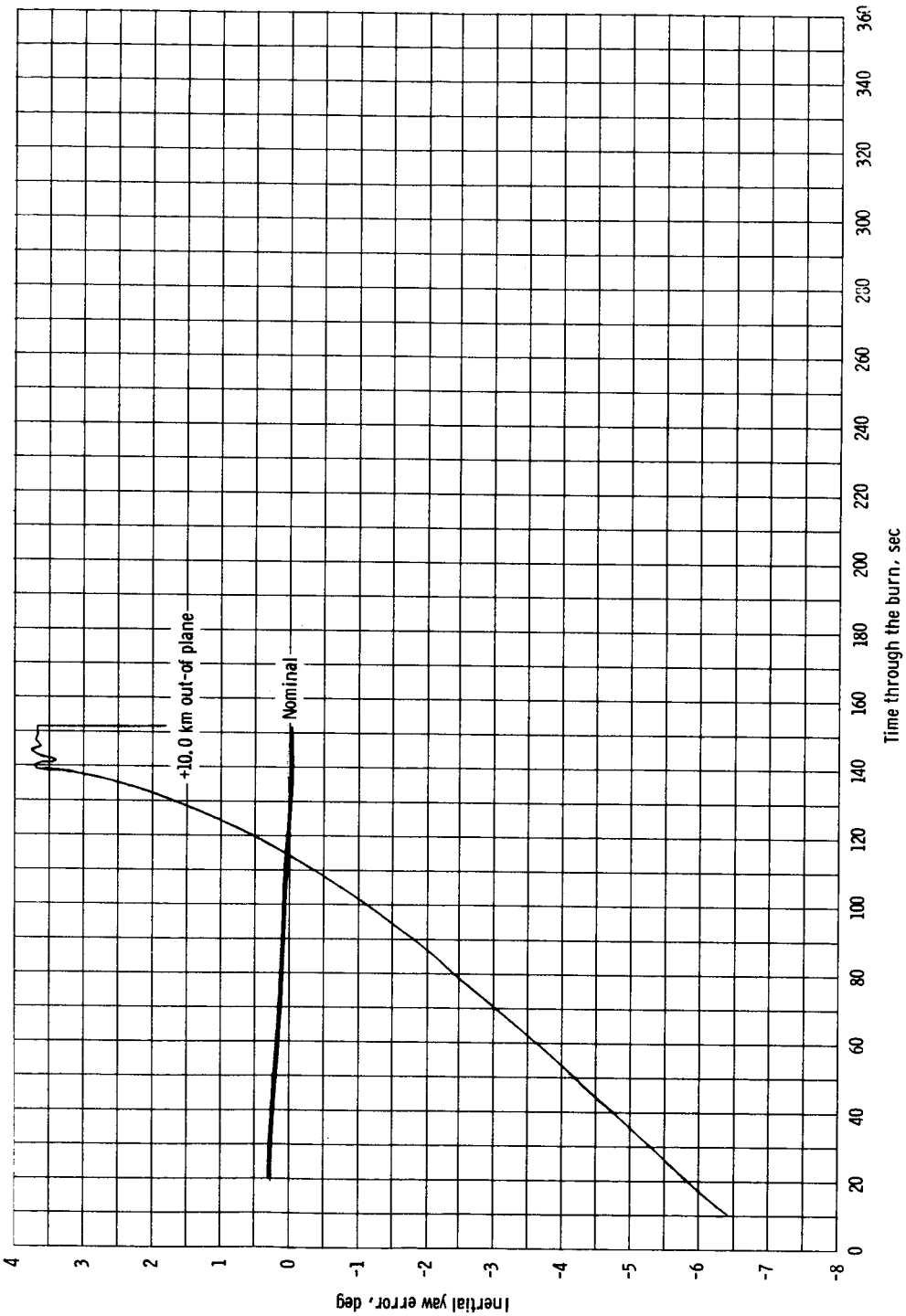

(b) Yaw error.

Figure 16. - Concluded.

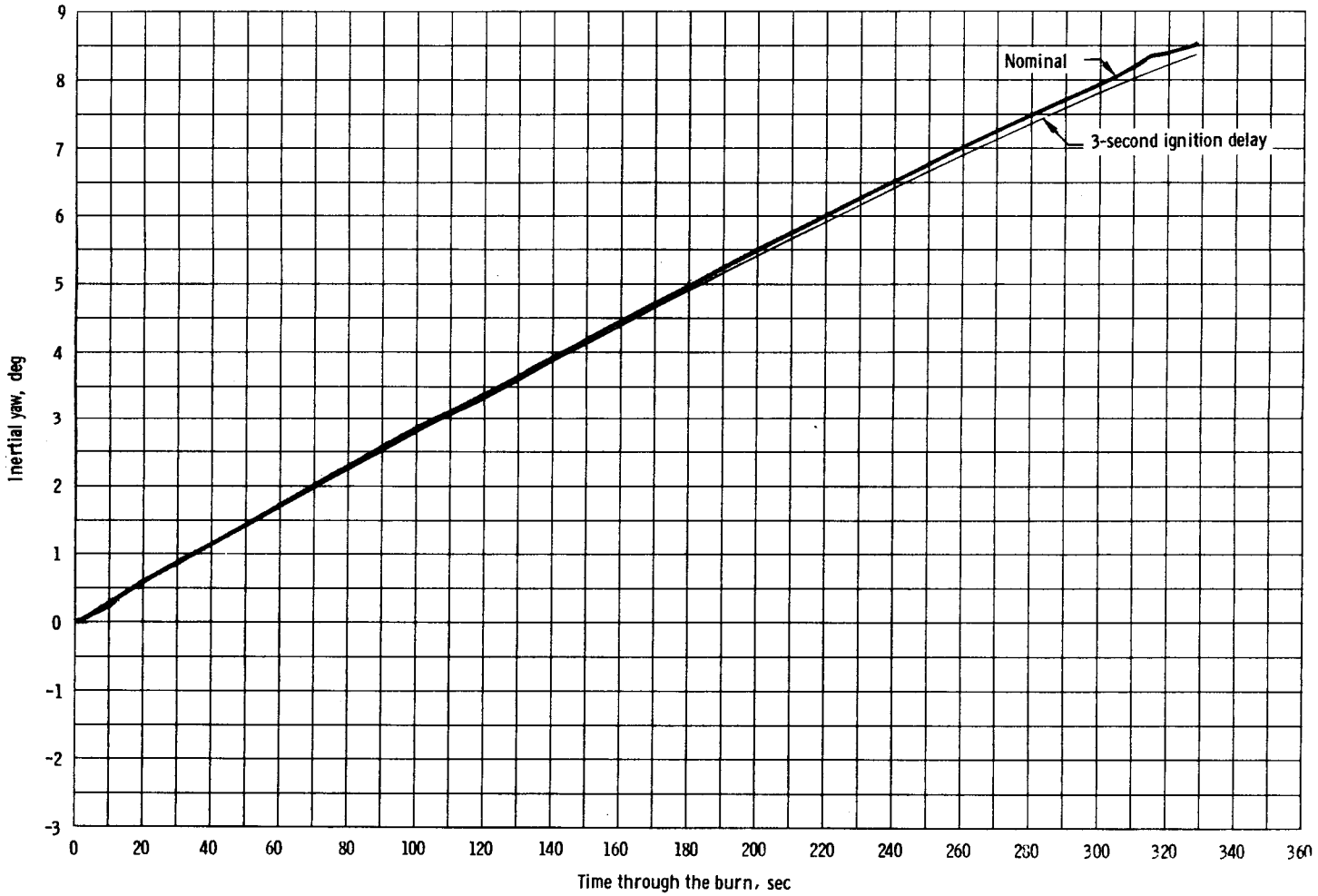

(a) Yaw.

Figure 17.- Inertial yaw and yaw error histories for a 3-second ignition delay in Mission G.

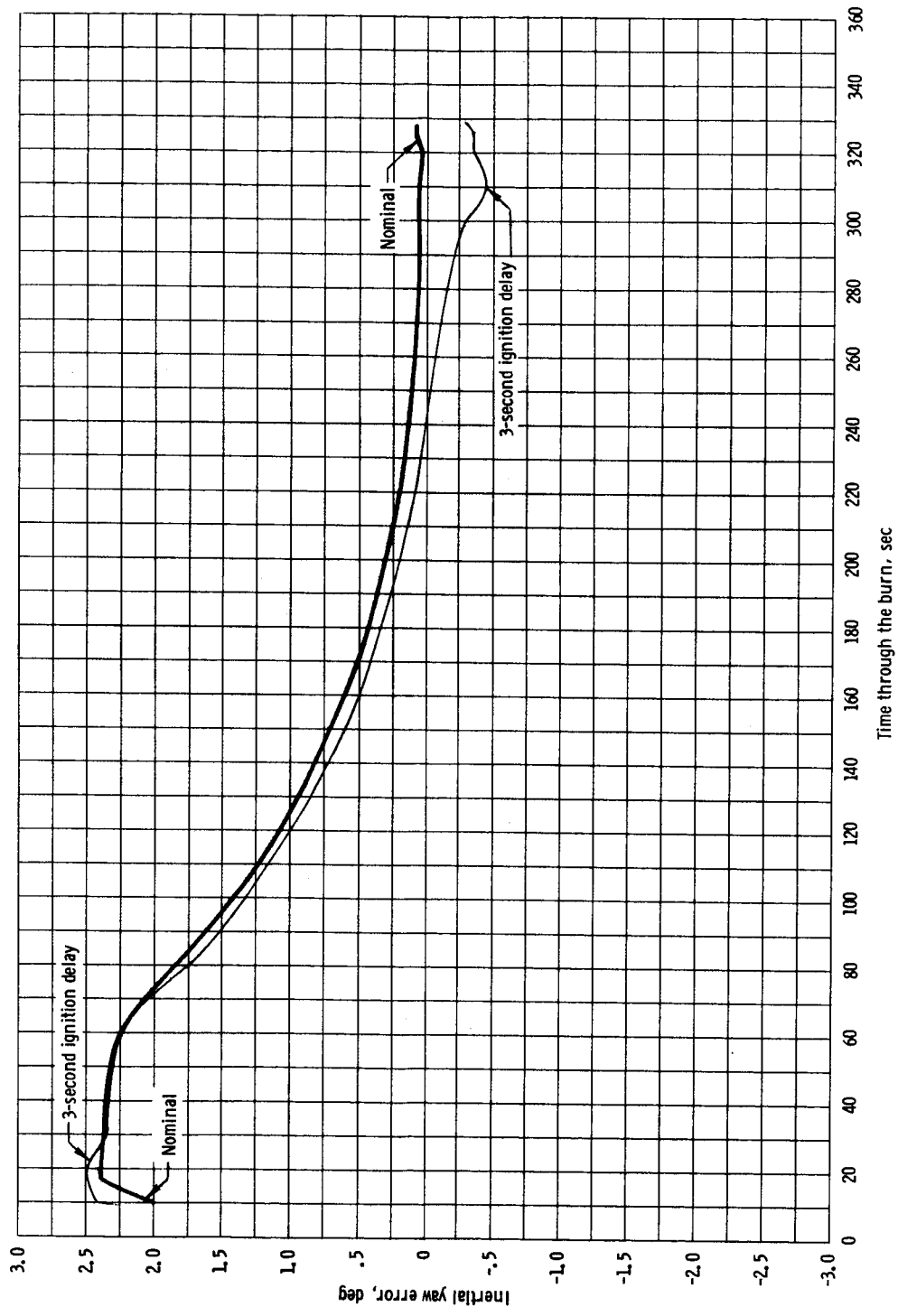

(b) Yaw error.

Figure 17. - Concluded.

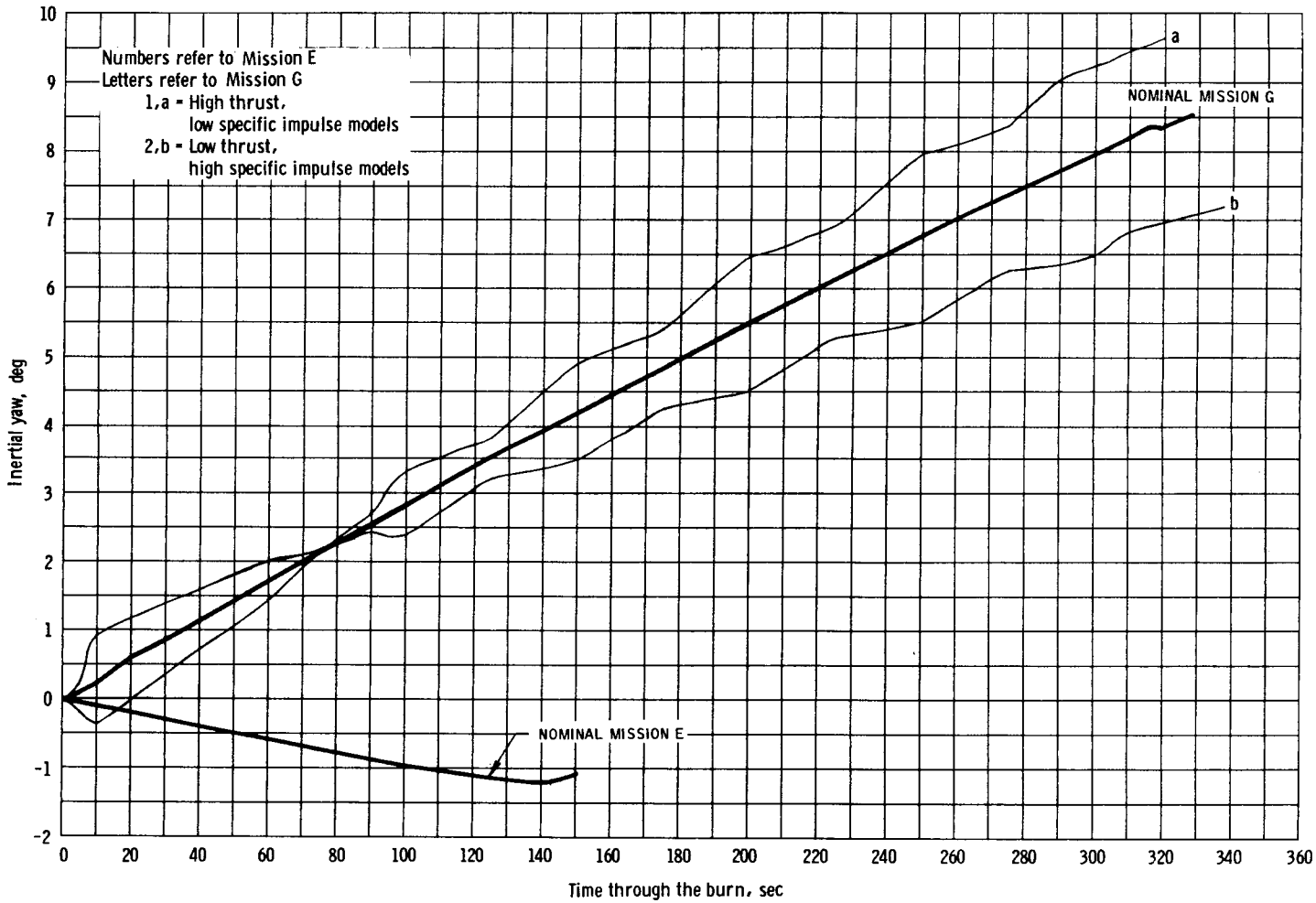

(a) Yaw for the two thrust and specific impulse models for Mission G.

Figure 18. - Inertial yaw and yaw error histories.

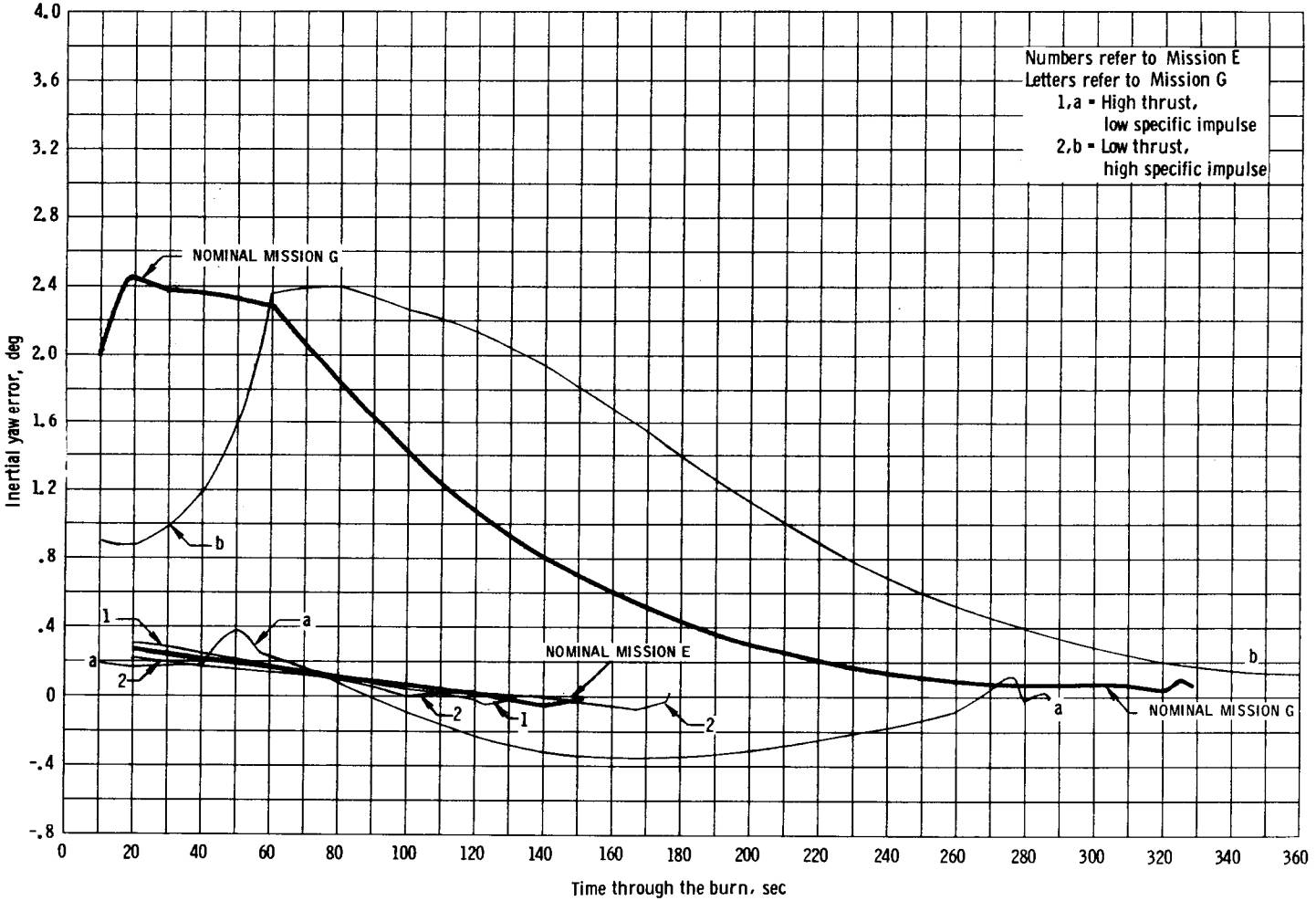

(b) Yaw error for constant thrust and specific impulse dispersions for Missions E and G.

Figure 18. - Concluded.

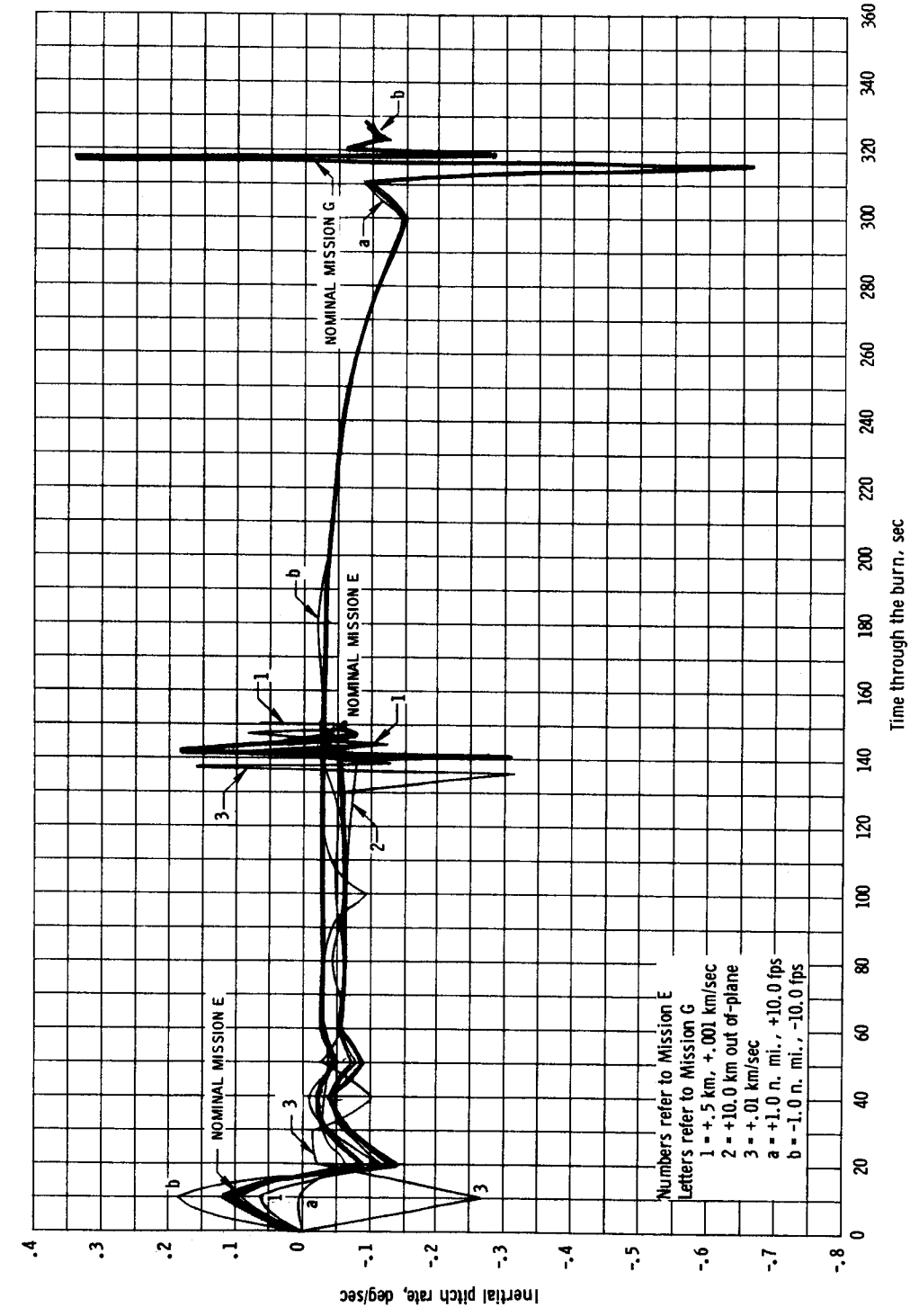

Figure 19.- Inertial pitch rate history for dispersed ignition states for Missions E and G.

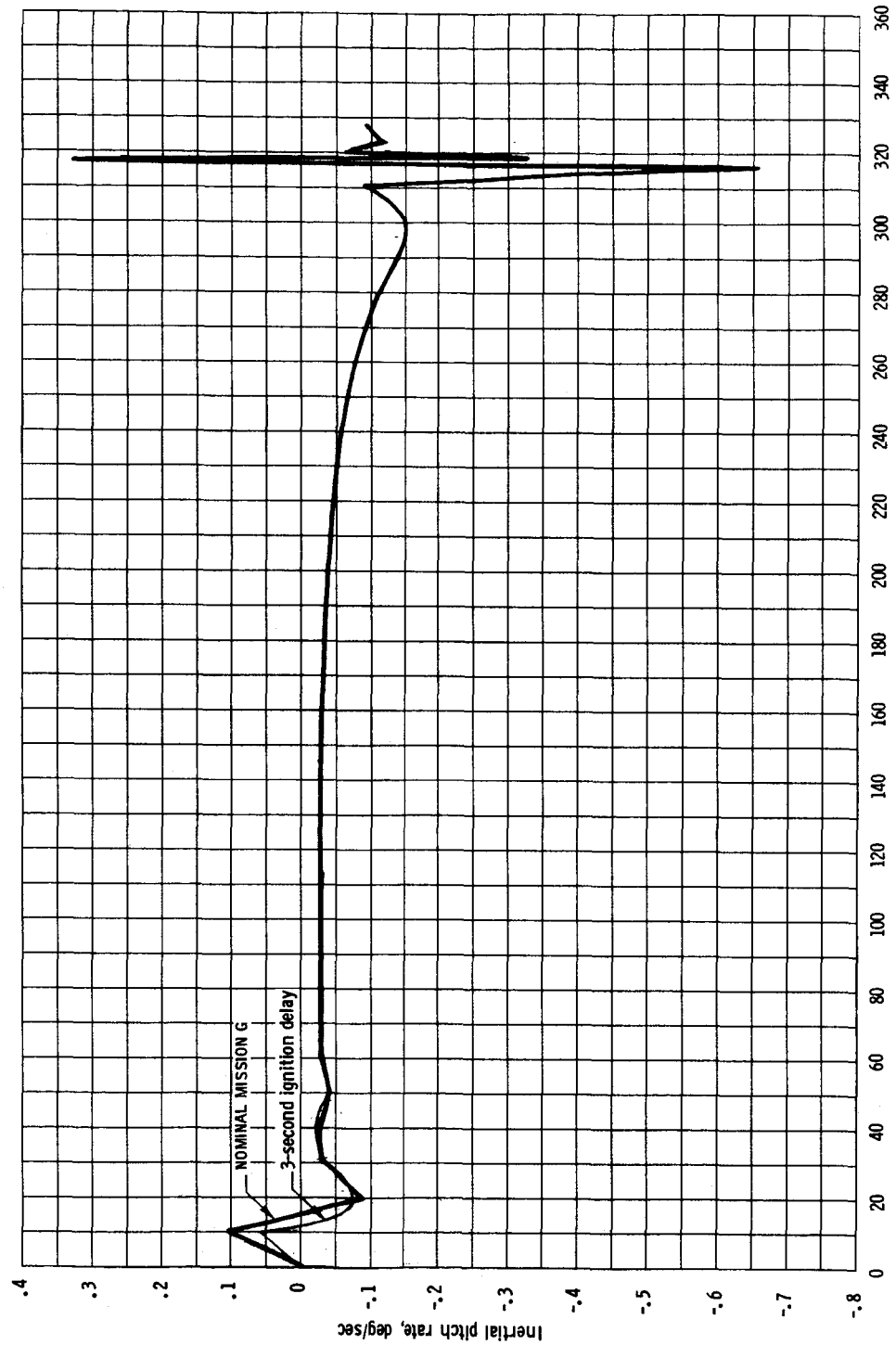

Figure 20.- Inertial pitch rate history for a 3-second ignition delay in Mission G.

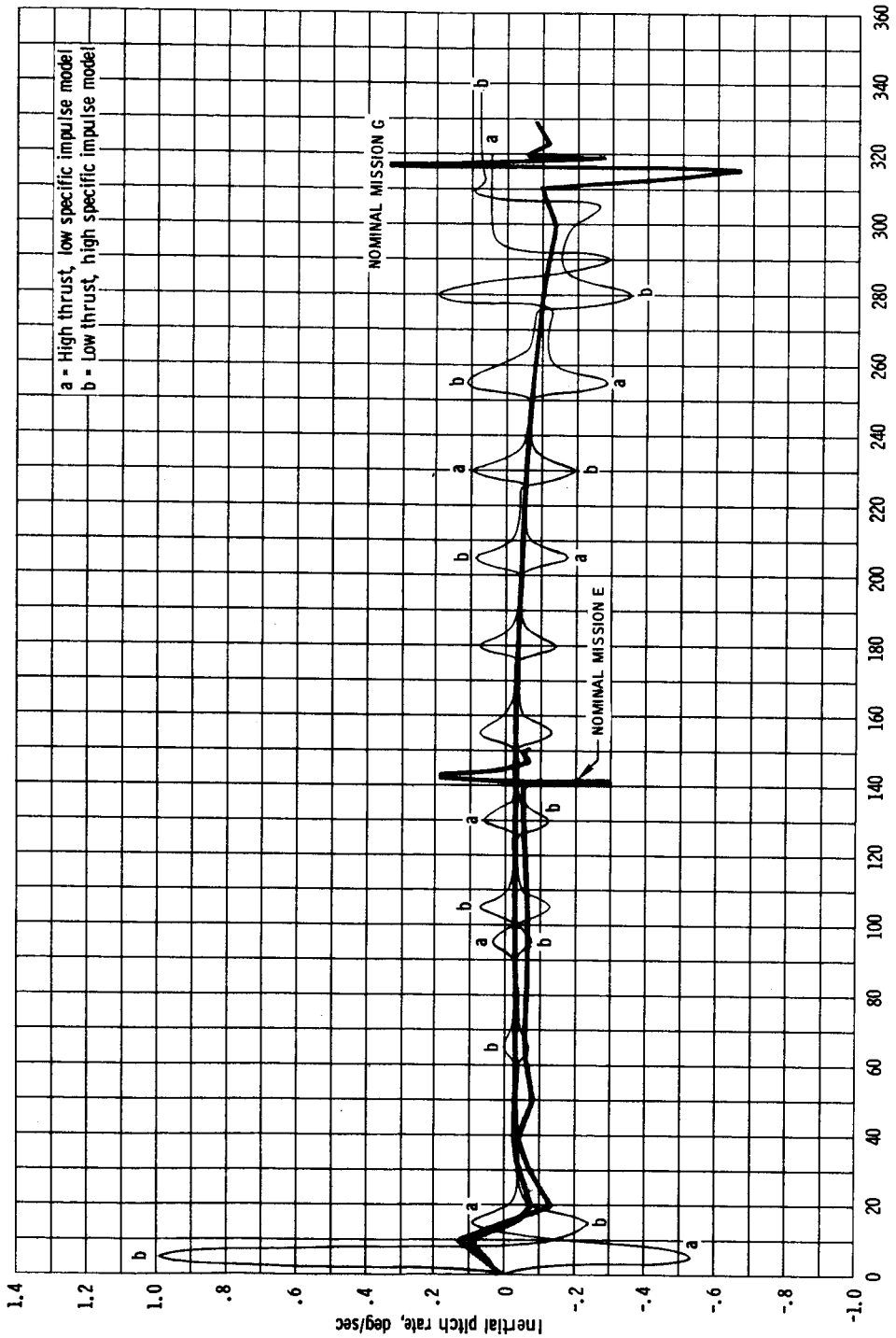

Figure 21 - Inertial pitch rate history for the two thrust and specific impulse models in Mission G.

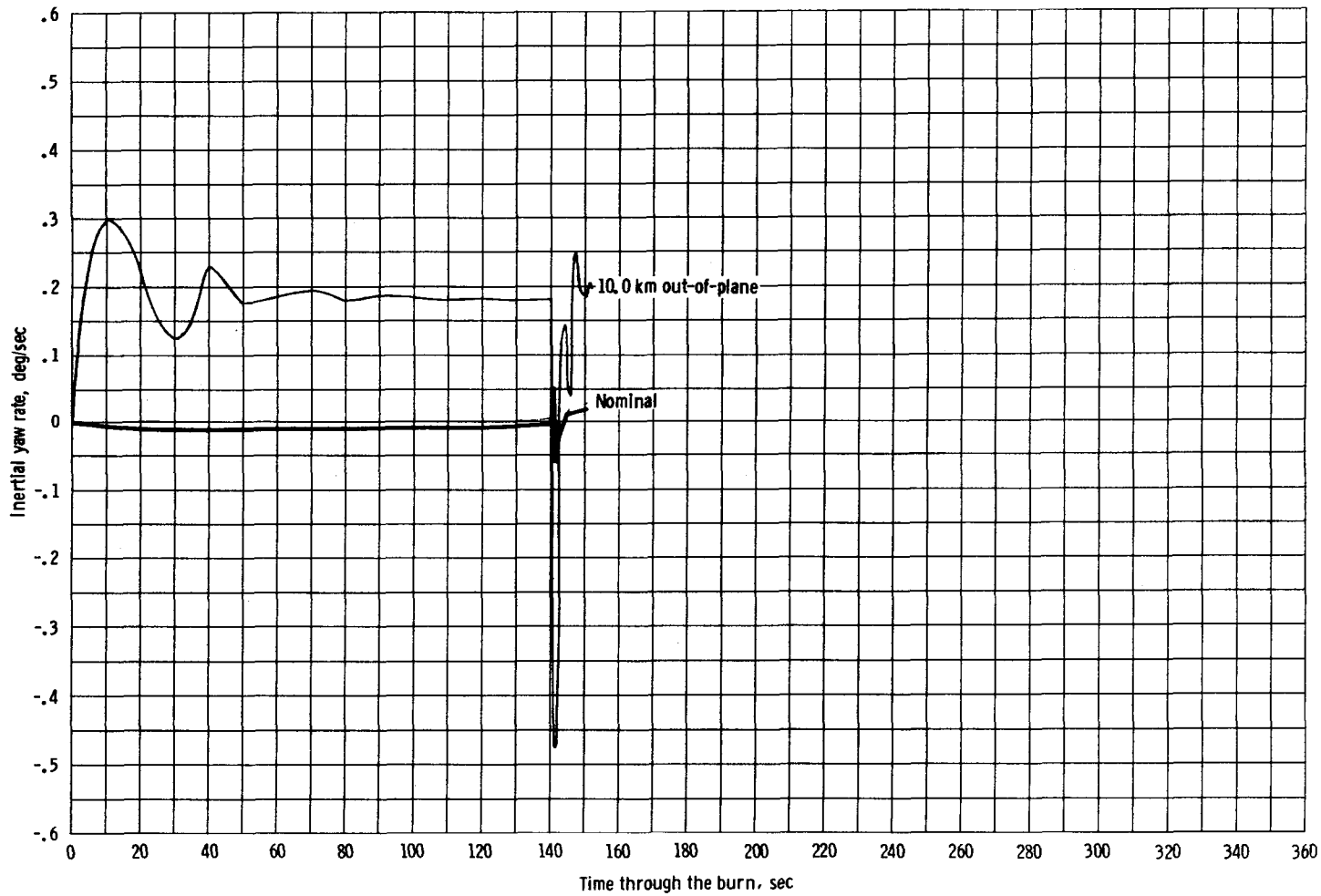

Figure 22. - Inertial yaw rate history for an out-of-plane position dispersion of the ignition state in Mission E.

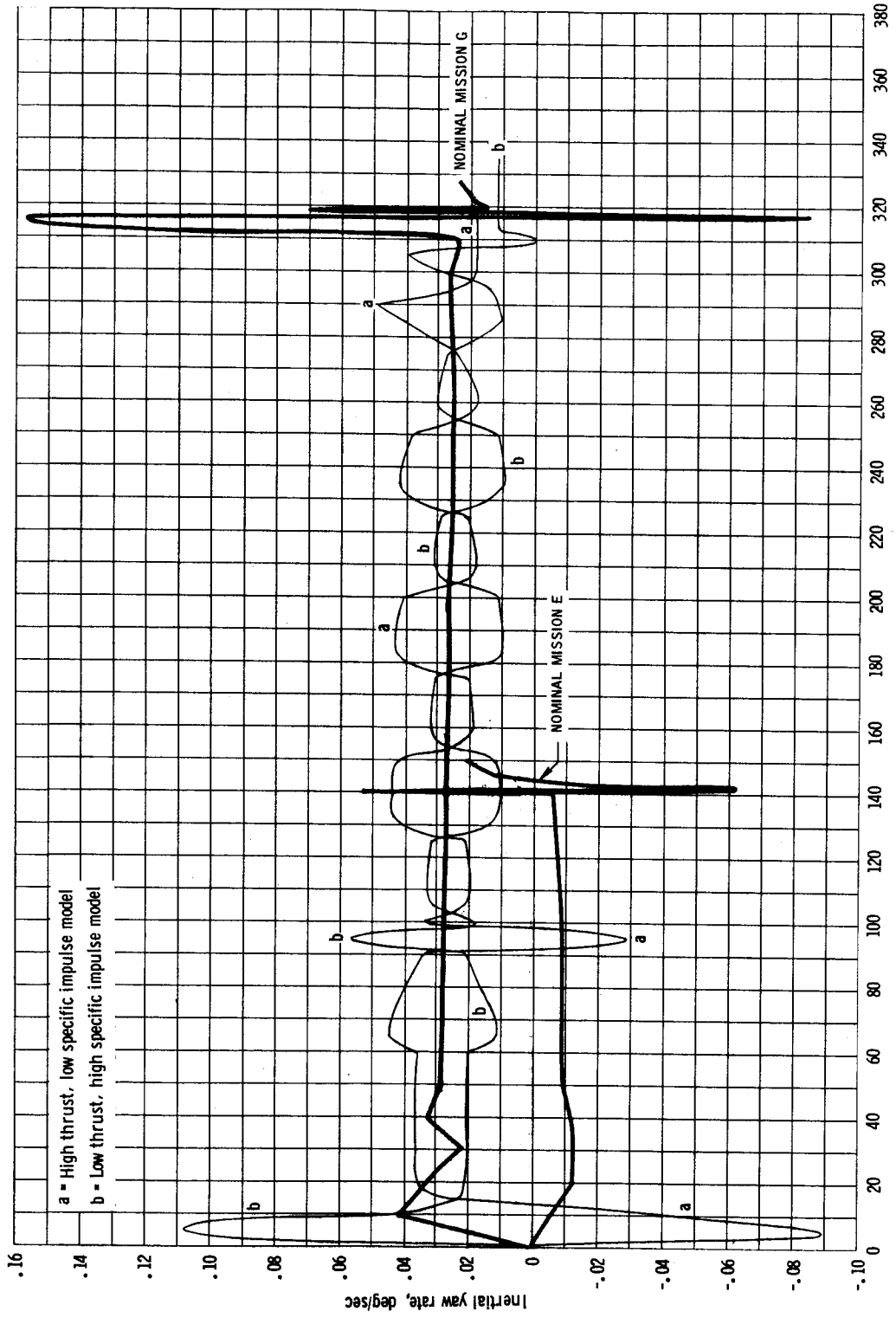

Figure 23. - Inertial yaw rate history for the two thrust and specific impulse models for Mission G.

REFERENCES

1. MITIL: Display During Boost Into Orbit. Space Guidance Analysis Memo No. 6-65. April 21, 1965.

2. MITIL: Attitude Errors During Boost and Transients During Boost Take-Over. Space Guidance Analysis Memo No. 16-65. November 9, 1965.

3. MITIL: Recent TVC DAP Changes. Flight 258 Memo No. 59. August 21, 1967.

4. McCaffety, Brody O.; Sellers, Donald R.; and Yencharis, Jerome D.: AS-503A/AS-504A Requirements for the RTCC: Translunar Injection Processor. MSC IN No. 67-FM-90, June 29, 1967.

5. Wiley, Robert F.: Use of Impulsive Targeting During AS-503A for a Spacecraft-Controlled Simulated Translunar Injection Burn. MSC IN No. 67-FM-118, August 15, 1967.